PHYSICAL REVIEW D **87,** 085028 (2013)

One-loop renormalization and the *S* matrix

Yu-tin Huang,[1,2] David A. McGady,[3] and Cheng Peng[4]

[1]*Department of Physics and Astronomy, University of California, Los Angeles, Los Angeles, California 90095, USA*
[2]*School of Natural Sciences, Institute for Advanced Study, Princeton, New Jersey 08540, USA*
[3]*Department of Physics, Princeton University, Jadwin Hall, Princeton, New Jersey 08544, USA*
[4]*Department of Physics, Michigan Center for Theoretical Physics, University of Michigan, Ann Arbor, Michigan 48109, USA*

(Received 16 September 2012; published 16 April 2013)

In four-dimensional theories with massless particles, one-loop amplitudes can be expressed in terms of a basis of scalar integrals and rational terms. Since the scalar bubble integrals are the only UV divergent integrals, the sum of the bubble coefficients captures the one-loop UV behavior. In particular, in a renormalizable theory the sum of the bubble coefficients equals the tree-level amplitude times a proportionality constant that is related to the one-loop beta function coefficient β_0. In this paper, we study how this proportionality is achieved from the viewpoint of on-shell amplitudes. For n-point MHV amplitude in (super) Yang-Mills theory, we demonstrate the existence of a hidden structure in each individual bubble coefficient which directly leads to systematic cancellations within the sum of them. The origin of this structure can be attributed to the collinear poles within a two-particle cut. Due to the cancellation, the one-loop beta function coefficient can be identified as a sum over the residues of unique collinear poles in particular two-particle cuts. Using CSW recursion relations, we verify the generality of this statement by reproducing the correct proportionality factor from such cuts for n-point split-helicity N^{k}MHV amplitudes.

DOI: 10.1103/PhysRevD.87.085028 PACS numbers: 11.55.−m, 11.15.Bt, 11.55.Bq, 12.38.Bx

I. INTRODUCTION AND SUMMARY OF RESULTS

In four spacetime dimensions, integral reduction techniques [1–3] allow one to express one-loop gauge theory amplitudes in terms of rational functions and a basis of scalar integrals that includes boxes I_4, triangles I_3, and bubbles I_2 [2,4,5]:

$$A^{\text{1-loop}} = \sum_i C_4^i I_4^i + \sum_j C_3^j I_3^j + \sum_k C_2^k I_2^k + \text{rationals}. \tag{1.1}$$

Here the index i (j or k) labels the distinct integrals categorized by the set of momenta flowing into each corner of the box (triangle or bubble). In this basis, the scalar bubble integrals I_2^i are the only ultraviolet divergent integrals in four dimensions. Moreover, the UV divergences of the bubble integrals take the universal form

$$I_2^i = \frac{1}{(4\pi)^2}\frac{1}{\epsilon} + \mathcal{O}(1) \tag{1.2}$$

for all i. Thus the *sum of bubble coefficients* contains information on the ultraviolet behavior of the theory at one loop.

In field theory, renormalizability requires that the ultraviolet divergences of the theory at one loop can be removed by inserting a finite number of counterterms to the corresponding tree diagrams for the same process. We can also understand this renormalizability from the amplitude point of view. In terms of amplitudes, renormalizability implies that the ultraviolet divergence at one loop must be proportional to the tree amplitude. As we will see in detail below, this proportionality between tree amplitudes and the bubble coefficients, which encapsulate UV behavior of the theory, in renormalizable theories is cleanly illustrated in pure-scalar QFTs. In ϕ^4 theory, the bubble coefficient of the 4-point one-loop amplitude evaluates to the 4-point tree amplitude 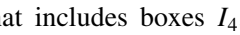 . However, in ϕ^5 theory, the bubble coefficient of the simplest one-loop amplitude evaluates to a new 6-point amplitude . Similarly, this new 6-point tree amplitude will generate higher-point tree structures at higher loops, which is the trademark of a nonrenormalizable theory.

This observation connects renormalizability with the one-loop bubble coefficient: in a renormalizable theory, the *sum of bubble coefficients* is proportional to the tree amplitude

$$\mathcal{C}_2 \equiv \sum_i C_2^i \propto A^{\text{tree}}, \tag{1.3}$$

where the sum i runs over all distinct bubble cuts, and we use the calligraphic $\mathcal{C}_2$ to denote the *sum* of the bubble coefficients. This proportionality relation takes a very simple form in (super) Yang-Mills [(S)YM] theory with all external lines being gluons [6–8] (see Ref. [9] for a detailed discussion)

$$\mathcal{C}_2 = -\beta_0 A_n^{\text{tree}}, \quad \beta_0 = -\left(\frac{11}{3}n_v - \frac{2}{3}n_f - \frac{1}{6}n_s\right), \tag{1.4}$$

where β_0 is the coefficient of the one-loop beta function and n_v, n_f, n_s are numbers of gauge bosons, fermions, and scalars, respectively. From the amplitude point of view, Eq. (1.4) appears to be a miraculous result as each

individual bubble coefficient is now a complicated rational function of Lorentz invariants. For example, it is shown in Refs. [9,10] that for the helicity amplitude $A_4(1^+2^-3^+4^-)$ in $\mathcal{N}$-fold super Yang-Mills theory, the bubble coefficients of the two cuts are

$$C_2^{(23,41)} = -(\mathcal{N}-4)\frac{\langle 12\rangle\langle 34\rangle}{\langle 13\rangle\langle 24\rangle}A_4^{\text{tree}}(1^+2^-3^+4^-), \quad \text{and}$$

$$C_2^{(12,34)} = -(\mathcal{N}-4)\frac{\langle 14\rangle\langle 23\rangle}{\langle 13\rangle\langle 24\rangle}A_4^{\text{tree}}(1^+2^-3^+4^-).$$

However, the sum of these two bubble coefficients is exactly proportional to the tree amplitude: $C_2^{(23,41)} + C_2^{(12,34)} = -(\mathcal{N}-4)A_4^{\text{tree}}(1^+2^-3^+4^-) = -\beta_0 A_4^{\text{tree}}(1^+2^-3^+4^-)$ by the Schouten identity. For an arbitrary n-point amplitude, Eq. (1.4) implies cancellation among a large number of these rational functions, in the end yielding a simple constant multiplying A_n^{tree}. The fact that the proportionality in Eq. (1.4) holds for any renormalizable theory hints at possible hidden structures in the sum of the bubble coefficients. Note that for gauge theories with nonadjoint matter fields, the individual bubble coefficients will also depend on higher-order Casimir invariants [10]. Renormalizability then requires all the higher-order invariants to cancel in the sum, leaving behind only the quadratic Casimir $tr_R(T^aT^b)$. In this paper, we seek to partially expose hidden structure of the bubble coefficients that leads to the proportionality to the tree amplitude.

Following Refs. [8,11], we extract the bubble coefficient by identifying it as the contribution from the pole at infinity in the complex z plane of a BCFW deformation [12] of the two internal momenta in the two-particle cut, where the complex deformation is introduced on the internal momenta. We begin with scalar theories as a warm-up. Here the contributions to bubble coefficients are tractable using Feynman diagrams in the two-particle cut. For scalar ϕ^n theories, we demonstrate that the bubble coefficient only receives contributions from one-loop diagrams that have exactly two loop propagators. For each diagram, the contribution is proportional to a tree diagram with a new $2(n-2)$-point interaction vertex. Renormalizability requires $n = 2(n-2)$, so this implies the familiar result, $n = 4$.

Feynman diagrams become intractable in gauge theories and it is simpler to use helicity amplitudes in the cut. In (super) Yang-Mills theory, we study general MHV n-point amplitudes and find that for each two-particle cut, the bubble coefficient can be separated into four separate terms. Each term stems from the four distinct singularities, which appear as the loop momenta become collinear to one of the adjacent external legs indicated in Fig. 1(a). We show that these singularities localize the Lorentz invariant phase space (dLIPS) integral to residues at four separate poles. Once given in this form, we find the following.

(i) For each collinear residue in a generic cut, there is a residue in the adjacent cut that has the same form but with opposite sign. When we sum over all channels, residues stemming from common collinear poles (CCP) in *adjacent* channels cancel pairwise, as indicated in Fig. 1. The sum therefore telescopes to four unique poles that come from four distinct "terminal cuts." Here we define a terminal cut as the two-particle cut which contains at least one 4-point tree amplitude on one side of the cut. The poles of interest correspond to the point in the phase space

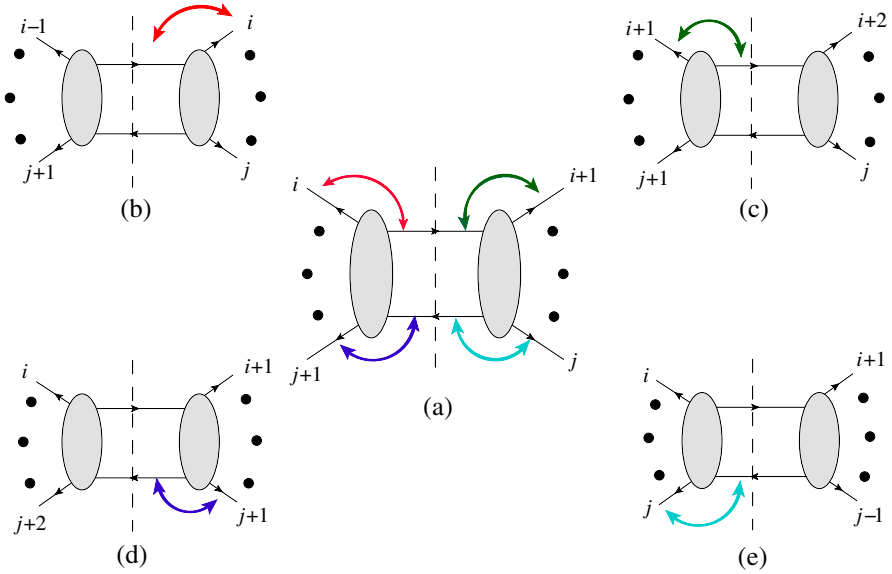

FIG. 1 (color online). A schematic representation of the cancellation of common collinear poles (CCP). The bubble coefficient of the cut in figure (a) receives contributions from the four collinear poles indicated by colored arrows. Each collinear pole is also present, with the opposite sign residues, in the corresponding adjacent cut indicated in figures (b), (c), (d), and (e), respectively. In the sum of bubble coefficients such contributions cancel in pairs.

where the two on-shell loop momenta become collinear with the two external scattering states in the 4-point subamplitude. We will refer to these poles as "terminal poles."

(ii) Focusing on the terminal poles we find that their contributions to the bubble coefficients are nontrivial only if the helicity configuration of the particles crossing the cut is "preserved," i.e., the loop helicity configuration is the same as the external lines on the 4-point tree amplitude as shown in Fig. 2. Thus the beta function of (super) Yang-Mills theory is given by the residues of the helicity conserving terminal poles.

For MHV amplitudes, we show that there are two nonvanishing terminal poles whose residues are identical and equal to $11/6A_n^{\text{tree}}$. Summing the two then gives the desired result $\mathcal{C}_2 = 11/3A_n^{\text{tree}}$ for the pure Yang-Mills (YM) theory, in agreement with Eq. (1.4). The relation (1.4) is also derived in the super Yang-Mills theory where $\mathcal{C}_2 = -(\mathcal{N}-4)\mathcal{A}_n^{\text{tree}}$ for $\mathcal{N} = 1, 2$.

For general N^{k}MHV split-helicity amplitudes in pure Yang-Mills theory, we also show that the residue of each helicity conserving terminal pole give $11/6A_n^{\text{tree}}$. We demonstrate this by using the CSW [13] representation for the N^{k}MHV tree amplitudes appearing in the two-particle cut. The fact that these terminal cuts give the correct proportionality factor indicates that these are indeed the only nontrivial contributions to the sum of bubble coefficients. This also hints that systematic cancellation in the sum of the bubble coefficients should be a property of Yang-Mills amplitude for the general helicity configuration. We give supporting evidence by using the collinear splitting function to show that the residues of CCP in a two-particle cut for generic gauge theories are indeed identical with opposite signs.

Our paper is organized as follows. In Sec. II, we compute the bubble coefficients for theories of self-interacting scalar fields, and rederive the well-known renormalizability conditions. We proceed to analyze (super) Yang-Mills theories with emphasis on the cancellation of CCP in Sec. III. We will use super Yang-Mills MHV amplitudes as the simplest demonstration of such cancellation. Similar results occur for MHV amplitudes in Yang-Mills as well. In Sec. IV, we give an argument for the cancellation of CCP for generic external helicity configurations by showing, using splitting functions of the tree amplitude in the cut, that the residue of collinear poles of the entire cut is indeed shared with an adjacent channel. We present further evidence in Sec. V by explicitly proving that the forward limit poles for split-helicity N^{k}MHV amplitudes indeed give the complete rhs of Eq. (1.4), implying complete cancellation of all other contributions.

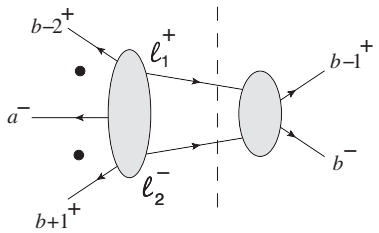

FIG. 2. The terminal channels that give nontrivial contribution to the sum of bubble coefficients. Note the helicity configurations of the loop legs of the n-point tree amplitude are identical with the two external legs on the 4-point tree amplitude in the cut.

II. BUBBLE COEFFICIENTS IN SCALAR FIELD THEORIES

As a toy model, we consider scalar theories with single interaction vertex $\alpha_k\phi^k$ in this section. It was shown in Ref. [8], following previous work in Ref. [11], that the bubble coefficient for a given two-particle cut can be calculated as

$$C_2^{(i,j)} = \frac{1}{(2\pi i)^2}\int d\text{LIPS}[l_1, l_2]\int_{\mathcal{C}}\frac{dz}{z}\hat{S}_n^{(i,j)}, \tag{2.1}$$

where (i, j) indicates the momentum channel $P = p_{i+1} + \cdots + p_j$ of the cut as shown in Fig. 7, $\hat{S}_n^{(\text{i,j})} = \hat{A}_L^{\text{tree}}(|\hat{l}_1\rangle, |\hat{l}_2]\hat{A}_R^{\text{tree}}(|\hat{l}_1\rangle, |\hat{l}_2])$, and $d\text{LIPS} = d^4l_1 d^4l_2\delta^{(+)}(l_1^2)\delta^{(+)}\times(l_2^2)\delta^4(l_1 + l_2 - P)$. Here $\hat{A}_{L,R}^{\text{tree}}$ in (2.1) are the amplitudes on either side of the cut; hats in (2.1) indicate a BCFW shift [12] of the two cut loop momenta:

$$\hat{l}_1(z) = l_1 + qz, \qquad \hat{l}_2(z) = l_2 - qz, \quad \text{with} \quad q\cdot q = q\cdot l_1 = q\cdot l_2 = 0. \tag{2.2}$$

We integrate the shift parameter z along a contour $\mathcal{C}$ that goes around infinity, which evaluates to the residue at the $z = \infty$ pole of the integrand.[1]

In a scalar theory, the only z dependence in BCFW-shifted tree amplitudes comes from propagators which depend on one of the two loop momenta. Under BCFW deformations, propagators of this type scale as $\sim 1/z$ for large z. Diagrams containing such propagators die off as $1/z$ or faster. The only nonvanishing contribution to the bubble coefficient comes from diagrams with the two shifted lines on the same vertex [14]. In this case there is neither z dependence nor dependence on l_1, or l_2 in the double cut and (2.1) evaluates to

$$C_2^{(i,j)} = -\frac{1}{2\pi i}\int d\text{LIPS}A_L^{\text{tree}}A_R^{\text{tree}} = A_L^{\text{tree}}A_R^{\text{tree}}, \tag{2.3}$$

[1]The BCFW shifts of the two-particle cut allow one to explore all possible on-shell realizations of a double cut for a given set of kinematics. The presence of finite-z poles indicates the existence of additional propagators, which are the contributions of box or triangle integrals to the double cut. The contribution from the bubble integrals then corresponds to poles at $z = \infty$, hence the choice of contour.

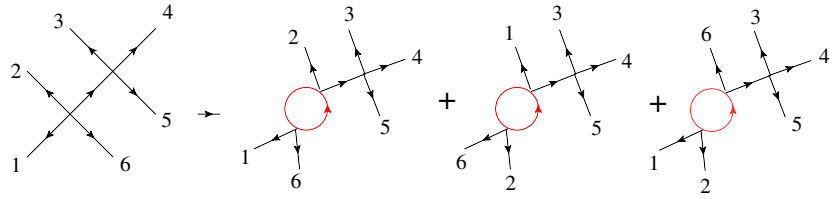

FIG. 3 (color online). For any given tree diagram in the ϕ^4 theory, each vertex can be blown up into 4-point one-loop subdiagrams in three distinct ways, while preserving the tree graph propagators. Each case contributes a factor of α_4 times the original tree diagram to the bubble coefficient. In this figure we show the example of 6-point amplitude.

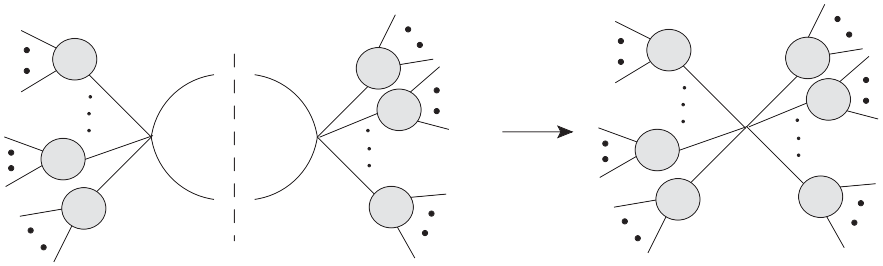

FIG. 4. For pure ϕ^k theory, the only one-loop diagrams that give nontrivial contribution to the bubble integrals are those with only two loop propagator. The contribution to the bubble coefficient is simply the product of the tree diagrams on both sides of the cut connected by a new $2(k-2)$ vertex.

where $A^{\text{tree}}_{L,R}$ are the unshifted amplitudes on either side of the cut as in Fig. 4, and we have used $\frac{1}{2\pi i}\int d\text{LIPS}(1) = -1$ (Appendix A). The bubble coefficient (1.3) is a sum over all cuts.

At 4-point, the tree amplitude is $A^{\text{tree}}_4 = \alpha_4$. There are two cuts of the one-loop 4-point amplitudes, namely the s and t channels. Then (2.3) gives

$$\begin{aligned}\mathcal{C}_2 &= A^{\text{tree}}_4(1,2,\hat{l}_1,\hat{l}_2)\times A^{\text{tree}}_4(-\hat{l}_2,-\hat{l}_1,3,4)\\ &\quad + A^{\text{tree}}_4(4,1,\hat{l}_1,\hat{l}_2)\times A^{\text{tree}}_4(-\hat{l}_2,-\hat{l}_1,2,3)\\ &= \alpha_4^2+\alpha_4^2 = 2\alpha_4 A^{\text{tree}}_4. \end{aligned} \tag{2.4}$$

This analysis extends to all n in ϕ^4 theory: each bubble cut with nonvanishing large-z pole will be precisely of this form. Evaluating the pole at infinity, and integrating over phase space reproduces a tree diagram. A semidetailed analysis reveals that, somewhat unsurprisingly, the tree diagrams generated in this way correctly reproduce (a result which is) proportional to the original tree amplitude,

$$C_2^{(n)}|_{\phi^4} = \frac{3(n-2)}{2}\,\alpha_4 A^n_{\text{tree}}. \tag{2.5}$$

A sketch of how this procedure is implemented, in practice, is depicted in Fig. 3.

One can do a similar analysis to the Yukawa theory with complex scalars. Here, Yukawa theory has asymptotic states of nonzero helicity; the analysis is somewhat aided through explicit use of tree-level helicity amplitudes, as opposed to an approach based solely on Feynman diagrams. Similar results hold. Details of this analysis are omitted here as Yukawa theory is well understood.

Crucial new aspects of and critical uses for integral reduction in conjunction with spinor-helicity technology manifest themselves in purest form in (S)YM. Use of spinor-helicity technology to describe tree amplitudes on either side of the bubble cut forces all gluons (and their supersymmetric cousins) to be on shell, and eliminates unphysical degrees of freedom from the calculation. As we shall see presently, this vastly simplifies calculations of the one-loop beta function in QCD [YM and (S)YM as well].

III. BUBBLE COEFFICIENTS FOR MHV (SUPER) YANG-MILLS AMPLITUDE

When we consider the (super) Yang-Mills theory, the proportionality between the sum of bubble coefficients and the tree amplitude becomes extremely nontrivial. Here, individual bubble coefficients are generically complicated rational functions of spinor inner products as illustrated for the $\langle\Phi_1\Psi_2\Phi_3\Psi_4\rangle$ case in the Introduction. In general, only after summing all the bubble coefficients and repeated use of Schouten identities will the result reduce to a simple constant times $\mathcal{A}^{\text{tree}}_n$. Thus from the amplitude point of view, this proportionality is a rather miraculous result.

In this section we show that the cancellation is in fact systematic. To see this, we show that for MHV amplitudes, the dLIPS integration will be localized by the collinear poles of the tree amplitude on both sides of the two-particle cut. For a generic cut, there are four distinct collinear poles involving the loop legs, each of which is also present in an adjacent cut, as illustrated in Fig. 5. It can be shown that the residues of these two adjacent cuts on their common

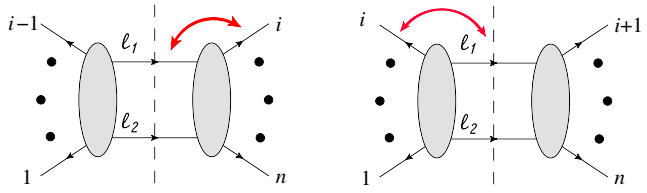

FIG. 5 (color online). An illustration of the cancellation between adjacent channels. The contribution to the bubble coefficient coming from the dLIPS integral evaluated around the collinear pole $\langle l_1 i\rangle \to 0$ indicated by the (red) arrows of the two diagrams cancels as indicated in Eq. (3.18).

collinear pole $\langle \lambda, i\rangle \to 0$ are exactly equal and with opposite sign. By separating the bubble coefficient into four different terms corresponding to contributions from four different poles, the cancellation between CCP in the sum of bubble coefficients is manifest.

Cancellation stops at "terminal cuts" where a 4-point tree and an n-point tree appear on opposites sides of the cut. The uncanceled terms in these terminal cuts correspond to the residues of collinear poles where the two loop momenta become collinear with the external momenta of the two external legs on the 4-point amplitude, as illustrated in Fig. 6. Explicitly, for *adjoint* fields (vectors, fermions, and scalars), we see the sum of these "terminal poles" is

$$-\beta_0 A_n^{\text{tree}}(1^+ \ldots a^-, \ldots, b^- \ldots n^+) = \left(\frac{11}{3}n_v - \frac{2}{3}n_f - \frac{1}{6}n_s\right)\frac{\langle a, b\rangle^4}{\langle 1, 2\rangle \cdots \langle i, i+1\rangle \cdots \langle n, 1\rangle}, \tag{3.1}$$

for MHV amplitudes with $n-2$ positive-helicity gluons and negative-helicity gluons a and b [15]. In the following, we will demonstrate this for n-point MHV amplitudes in $\mathcal{N} = 1, 2$ super Yang-Mills theory. This systematic cancellation is also present for pure Yang-Mills MHV amplitudes (explicitly shown in Appendix B).

Before going further, we pause to note an important distinguishing feature between the bubble coefficients in scalar QFT and in (S)YM. Specifically, the proportionality constant in (super) Yang-Mills is independent of the number of external legs: it is just $-\beta_0$, the coefficient of the one-loop beta function. To see this note that for (super) Yang-Mills theory, there are diagrams with one-loop bubbles in the external legs. These massless bubbles do not appear in Eq. (1.1), as they are set to zero in dimensions regularization, reflecting the cancellation between collinear IR and UV divergences. However, when one is only considering the pure UV divergence of the amplitude, one must take into account the existence of the UV divergences in the external bubble diagrams, which are simply the same as that of the infrared divergences in the external bubbles but with a relative minus sign. Thus we have

$$A_n|_{\text{UV div.}} = \left(\sum C_{\text{bubble}} I_{\text{bubble}}\right)_{\text{UV}} + \text{UV}_{\text{ext. bubbles}} = \left(\sum C_{\text{bubble}} I_{\text{bubble}}\right)_{\text{UV}} - \text{IR}_{\text{ext. bubbles}}. \tag{3.2}$$

For n-gluon one-loop amplitudes, the collinear IR divergences take the form [6]

$$\text{IR: } A_{n,\text{collinear}}^{\text{1-loop}} = -\frac{g^2}{(4\pi)^2}\frac{1}{\epsilon}\frac{n}{2}\beta_0 A_n^{\text{tree}}. \tag{3.3}$$

At leading order in $\epsilon \to 0$, the UV divergence is [6]

$$\text{UV: } A_{n,\text{UV}}^{\text{1-loop}} = +\frac{g^2}{(4\pi)^2}\frac{1}{\epsilon}\left(\frac{n-2}{2}\right)\beta_0 A_n^{\text{tree}}. \tag{3.4}$$

Thus the bubble coefficients (total UV divergence) in *purely* gluonic one-loop amplitudes are

$$\sum_i C_2^i = A_{n,\text{UV}}^{\text{1-loop}} + A_{n,\text{collinear}}^{\text{1-loop}} = -\beta_0 A_n^{\text{tree}} = \frac{11}{3}A_n^{\text{tree}}. \tag{3.5}$$

At one loop, ϕ^4 scalar field theory lacks these collinear divergences on external legs, and no UV/IR mixing occurs, hence pure scalar bubble coefficients scale with $\frac{n-2}{2}$, the number of interaction vertices.

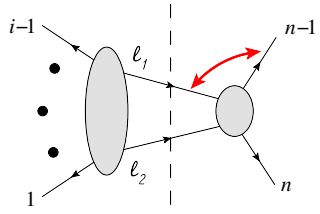

FIG. 6 (color online). The "terminal" pole that contributes to the bubble coefficient. Such poles appear in the two-particle cuts that have two legs on one side of the cut and one of the legs has to be a minus helicity. Note that, at this point in phase space, $l_1 = -p_{n-1}$ and $l_2 = -p_n$.

A. Extracting bubble coefficients in ($\mathcal{N} = 0, 1, 2$ super) Yang-Mills

The bubble coefficient for a given two-particle cut of a one-loop (S)YM amplitude is computed in essentially the same way as for scalar field theory. However, as emphasized in the Introduction, unlike the case for scalar QFT extracting this through Feynman diagrams is rather intractable. Roughly in YM this is because BCFW shifts of the two internal on-shell gluon lines in the double cut introduces z dependence in local interaction vertices *and* polarization vectors. These difficulties are only amplified in ($\mathcal{N} \neq 0$) SYM.

It is more efficient to directly express the left-hand and right-hand amplitudes as entire on-shell objects through the use of the spinor-helicity formalism. Here the dLIPS integration over allowed on-shell momenta is conveniently

converted into an integration over spinor variables which automatically solve the delta functions,

$$\int d^4l_1 d^4l_2 \delta^{(+)}(l_1^2)\delta^{(+)}(l_2^2)\delta^4(l_1+l_2-P)g(|l_1\rangle,|l_2\rangle)$$
$$=\int_{\tilde{\lambda}=\bar{\lambda}} P^2 \frac{\langle\lambda, d\lambda\rangle[\tilde{\lambda}, d\tilde{\lambda}]}{\langle\lambda|P|\tilde{\lambda}]^2} g(|\lambda\rangle, P|\tilde{\lambda}]), \tag{3.6}$$

where we have identified $|l_1\rangle = |\lambda\rangle$, $|l_2\rangle = P|\tilde{\lambda}]$, and $\int_{\tilde{\lambda}=\bar{\lambda}}$ indicates we are integrating over the real contour (real momenta).[2] The $\hat{S}_n^{(i,j)}$ in (2.1) takes the form

$$\hat{S}_n^{(i,j)} = \hat{S}_{n,0}^{(i,j)} \equiv \sum_{\text{state sum}} \hat{A}_L^{\text{tree}}(|\hat{l}_1\rangle,|\hat{l}_2]) \hat{A}_R^{\text{tree}}(|\hat{l}_1\rangle,|\hat{l}_2]), \tag{3.7}$$

in the Yang-Mills theory. Note that to fully integrate out the bubble coefficients' dependence on the internal lines, we sum over all possible states in the loop.

Further, extraction of simple bubble coefficients is aided by on-shell supersymmetry (SUSY).[3] Here amplitudes and state sums are promoted to superamplitudes and Grassmann integrals

$$\hat{S}_n^{(i,j)} = \hat{S}_{n,\mathcal{N}}^{(i,j)} \equiv \sum_\sigma \int d^{\mathcal{N}}\eta_{l_1} d^{\mathcal{N}}\eta_{l_2} \hat{\mathcal{A}}_{L\sigma}^{\text{tree}} \hat{\mathcal{A}}_{R\bar{\sigma}}^{\text{tree}}, \quad \mathcal{N}=1,2, \tag{3.8}$$

where σ labels the different pairs of multiplets that the loop legs l_1 and l_2 belong to. Following Ref. [9], on-shell states are encoded into two separate on-shell superfields, Φ and Ψ, that contain states in the "positive-" and "negative-helicity" sectors. In this language, $\{\sigma\} = \{(\Phi,\Psi),(\Psi,\Phi),(\Phi,\Phi),(\Psi,\Psi)\}$. The $\bar{\sigma}$ is the conjugate configuration of σ.

Crucially, to preserve SUSY the *bosonic* BCFW shift (2.2) must be combined with a *fermionic* shift of the Grassmann variables η^a [8,16]

$$|\hat{l}_1(z)\rangle = |l_1\rangle + z|l_2\rangle, \qquad |\hat{l}_2(z)] = |l_2] - z|l_1], \tag{3.9a}$$
$$\hat{\eta}_{l_2 a} = \eta_{l_2 a} + z\eta_{l_1 a}, \qquad a = 1,\ldots,\mathcal{N}. \tag{3.9b}$$

Note the bosonic shift (3.9a) is identical to the shift (2.2) when cast in terms of the spinor-helicity variables; it is referred to as an $[l_2, l_1\rangle$ shift.

Combined supershifts (3.9) of any tree amplitude of the $\mathcal{N}=4$ SYM fall off as $1/z$ for large z. In (S)YM theory with $\mathcal{N}=0,1,2$ supersymmetry, it was shown [9] that the super-BCFW shifts $[\Phi,\Phi\rangle$, $[\Psi,\Phi\rangle$, and $[\Psi,\Psi\rangle$ fall off as $1/z$ at large z while the $[\Phi,\Psi\rangle$ supershift grows as $z^{3-\mathcal{N}}$ for large z. For $\mathcal{N}=0$ pure Yang-Mills, this reduces to the familiar observation that for shifts $[-,-\rangle$, $[-,+\rangle$, and $[+,+\rangle$ the amplitudes fall off as $1/z$, while the $[+,-\rangle$ shifts grow as z^3 [12,17].

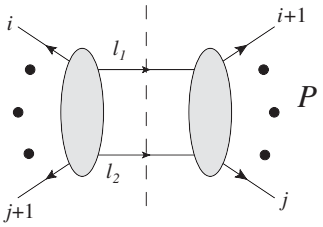

FIG. 7. A two-particle cut for a generic n-point amplitude.

Carrying out the z integral gives

$$C_2^{(i,j)} = -\frac{1}{2\pi i}\int d\text{LIPS}[l_1,l_2][\hat{\mathcal{S}}_{n,\mathcal{N}}^{(i,j)}]_{O(1)\text{ as }z\to\infty}, \quad \mathcal{N}=0,1,2, \tag{3.10}$$

where $[\hat{\mathcal{S}}_{n,\mathcal{N}}^{(i,j)}]_{O(1)\text{ as }z\to\infty}$ is the residue of $\hat{\mathcal{S}}_{n,\mathcal{N}}^{(i,j)}$ at the $z\to\infty$ pole.

Double cuts with internal states $\sigma\in\{(\Phi,\Phi),(\Psi,\Psi)\}$ shown in cut (a) of Fig. 8 scale as

$$\hat{\mathcal{S}}_{n,\mathcal{N}}^{[\text{Cut (a)}]} \sim \frac{1}{z}\times\frac{1}{z} \sim \frac{1}{z^2} \quad \text{as} \quad z\to\infty. \tag{3.11}$$

Cuts of this type do not contribute to the bubble coefficient. On the other hand, cuts with internal states $\sigma\in\{(\Phi,\Psi),(\Psi,\Phi)\}$, such as cut (b) in Fig. 8, always involve a shift that acts as $[\Psi,\Phi\rangle$ on one subamplitude and as $[\Phi,\Psi\rangle$ on the other. This gives

$$\hat{\mathcal{S}}_{n,\mathcal{N}}^{[\text{Cut (b)}]} \sim \frac{1}{z}\times z^{3-\mathcal{N}} \sim z^{2-\mathcal{N}} \quad \text{as} \quad z\to\infty. \tag{3.12}$$

Note that (3.12) indicates that there can be nonvanishing $O(1)$ terms and hence contributions to the sum of the bubble coefficients in $\mathcal{N}=0$, 1, 2 SYM but not in the $\mathcal{N}=4$ SYM theory. This is consistent with the known nonvanishing one-loop β functions in $\mathcal{N}=0$, 1, 2 SYM theories as well as the UV finiteness of $\mathcal{N}=4$ SYM.

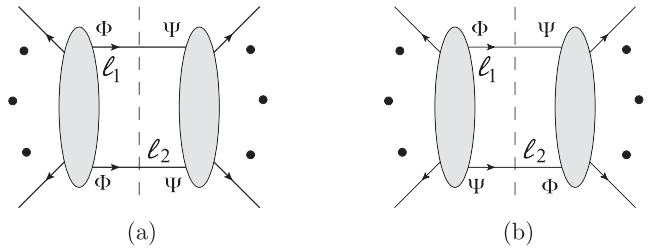

FIG. 8. Illustration of two internal helicity configurations of the cut loop momenta. (a) Cuts with $\sigma\in\{(\Phi,\Phi),(\Psi,\Psi)\}$ die off, and have no pole, as $z\to\infty$. (b) Cuts with $\sigma\in\{(\Phi,\Psi),(\Psi,\Phi)\}$ have a pole at $z\to\infty$.

[2]The explicit evaluation of integrals in Eq. (3.6) using the holomorphic anomaly [8,9,13] is reviewed in Appendix A.

[3]The calculations for the simplest bubble coefficients are simpler in $\mathcal{N}=1$, 2 SYM than in YM. To see this, compare nonadjacent MHV bubble computations in SYM (Sec. III B) and in YM (Appendix B).

We can also investigate the contribution to the bubble coefficients from particular states crossing the two-particle cut. These contributions can be projected out by acting with appropriate Grassmann integrations/derivatives on the above superamplitudes. By analyzing the large-z behavior of the integration measure, as shown in Ref. [9], we get the large-z behavior of the bubble coefficient of certain internal states. The implication for QCD with one flavor of fermions can simply be deduced from $\mathcal{N}=1$ super Yang-Mills, where there are no scalars in the multiplet. For example, a simple computation shows that a double cut of an internal negative-helicity gluino and an internal negative-helicity gluon exiting (entering) one of the two tree amplitudes does not contribute to the bubble coefficients in $\mathcal{N}=1$ SYM theory. Then following Ref. [18], this result is also true in QCD with one flavor of fermions. Note that the difference between fundamental and adjoint fermions is irrelevant for this analysis since we are interested in color-ordered amplitudes and the large-z behavior of the cut holds for individual internal helicity configurations and not the sum.

B. MHV bubble coefficients in $\mathcal{N}=1, 2$ super Yang-Mills theory

It was shown in Ref. [9], that for the MHV amplitudes in $\mathcal{N}=1$, 2 super Yang-Mills theory, the $\mathcal{O}(z^0)$ part of the BCFW-shifted two-particle cut $\hat{\mathcal{S}}^{(i,j)}_{\{a,b\},\mathcal{N}}$ depicted in Fig. 9 is given by

$$\hat{\mathcal{S}}^{(i,j)}_{\{a,b\},\mathcal{N}}|_{\mathcal{O}(z^0)} = (\mathcal{N}-4)\mathcal{A}_n^{\text{tree}}\frac{\langle i, i+1\rangle\langle j, j+1\rangle}{\langle a, b\rangle^2} \times \frac{\langle a, \lambda\rangle^2\langle b, \lambda\rangle^2}{\langle j, \lambda\rangle\langle j+1, \lambda\rangle\langle i, \lambda\rangle\langle i+1, \lambda\rangle}, \tag{3.13}$$

where $\{a, b\}$ indicates the positions of the two sets of external negative-helicity states (within the Ψ multiplets). We have set $|l_2\rangle = |\lambda\rangle$. Since $\hat{\mathcal{S}}^{(i,j)}_{\{a,b\},\mathcal{N}}$ is purely holomorphic in λ, we can straightforwardly use Eq. (A2) to rewrite the dLIPS integral (3.6) as a total derivative, and the bubble coefficient is given as

$$\begin{aligned} C^{(i,j)}_{2\{a,b\}} &= \frac{-1}{2\pi i}\oint_{\tilde{\lambda}=\bar{\lambda}} P^2_{i+1,j}\frac{\langle\lambda, d\lambda\rangle[\tilde{\lambda}, d\tilde{\lambda}]}{\langle\lambda|P_{i+1,j}|\tilde{\lambda}]^2}\hat{\mathcal{S}}^{(i,j)}_{\{a,b\},\mathcal{N}}|_{\mathcal{O}(z^0)} \\ &= \frac{1}{2\pi i}\oint_{\tilde{\lambda}=\bar{\lambda}}\langle\lambda, d\lambda\rangle d\tilde{\lambda}_{\dot{\alpha}}\frac{\partial}{\partial\tilde{\lambda}_{\dot{\alpha}}} \\ &\quad\times\left[\frac{[\tilde{\lambda}|P_{i+1,j}|\alpha\rangle}{\langle\lambda|P_{i+1,j}|\tilde{\lambda}]\langle\lambda, \alpha\rangle}\hat{\mathcal{S}}^{(i,j)}_{\{a,b\},\mathcal{N}}|_{\mathcal{O}(z^0)}\right], \end{aligned} \tag{3.14}$$

where $|\alpha\rangle$ is an auxiliary reference spinor. In this section, for convenience, we label the bubble coefficients $C^{(i,j)}_{2\{a,b\}}$ in the same way as the two-particle cut $\hat{\mathcal{S}}^{(i,j)}_{\{a,b\},\mathcal{N}}$. There are two kinds of poles inside the total derivative: the four collinear poles of $\hat{\mathcal{S}}^{(i,j)}_{\{a,b\},\mathcal{N}}$ in Eq. (3.13) and the spurious pole $1/\langle\lambda, \alpha\rangle$. The spurious pole can be simply removed by the $\langle a, \lambda\rangle^2\langle b, \lambda\rangle^2$ factor in the numerator of Eq. (3.13) if we choose the auxiliary spinor $|\alpha\rangle$ to be $|a\rangle$ or $|b\rangle$. Thus with this choice of reference spinor, the contributions to the bubble coefficient come solely from the collinear poles in $\hat{\mathcal{S}}^{(i,j)}_{\{a,b\},\mathcal{N}}|_{\mathcal{O}(z^0)}$.

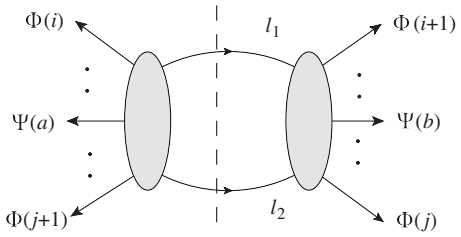

FIG. 9. The two-particle cut that gives $\hat{\mathcal{S}}^{(i,j)}_{\{a,b\},\mathcal{N}}$.

From Eq. (3.13) we see that there are four collinear poles in $\hat{\mathcal{S}}^{(i,j)}_{\{a,b\},\mathcal{N}}|_{\mathcal{O}(z^0)}$, each corresponding to λ becoming collinear with the adjacent external lines of the cut. Careful readers might find this puzzling, as the MHV tree amplitudes on both sides of the cut only have collinear poles of the form $\langle l_1, i\rangle$, $\langle l_1, i+1\rangle$, $\langle l_2, j\rangle$, and $\langle l_2, j+1\rangle$. Recalling that here $|\lambda\rangle = |l_2\rangle$, one would instead expect collinear poles of the form $[\lambda|P_{i+1,j}|i\rangle$, $[\lambda|P_{i+1,j}|i+1\rangle$, $\langle\lambda, j\rangle$, and $\langle\lambda, j+1\rangle$. The resolution is that Eq. (3.13) is obtained by shifting $\langle l_1, i\rangle \to \langle l_1, i\rangle + z\langle l_2, i\rangle$ and expanding around $z\to\infty$, thus introducing the $\langle l_2, i\rangle$ poles:

$$\frac{1}{\langle l_1(z), i\rangle}\bigg|_{z\to\infty} = \frac{1}{z\langle l_2, i\rangle} + \mathcal{O}\left(\frac{1}{z^2}\right). \tag{3.15}$$

Since these poles originated from $\langle l_1(z), i\rangle$, we will abuse the terminology, as well as the figures, and still refer to them as collinear poles.[4]

To better track the contributions of the collinear poles, we rewrite the integrand as follows:

$$\begin{aligned} \hat{\mathcal{S}}^{(i,j)}_{\{a,b\},\mathcal{N}}|_{\mathcal{O}(z^0)} &= (\mathcal{N}-4)\mathcal{A}_n^{\text{tree}}\frac{\langle a, \lambda\rangle\langle b, \lambda\rangle^2\langle i, i+1\rangle}{\langle a, b\rangle^2\langle i, \lambda\rangle\langle i+1, \lambda\rangle} \\ &\quad\times\left(\frac{\langle a, j+1\rangle}{\langle j+1, \lambda\rangle} - \frac{\langle a, j\rangle}{\langle j, \lambda\rangle}\right) \\ &= (\mathcal{N}-4)\mathcal{A}_n^{\text{tree}}\frac{\langle a, \lambda\rangle\langle b, \lambda\rangle^2\langle j, j+1\rangle}{\langle a, b\rangle^2\langle j, \lambda\rangle\langle j+1, \lambda\rangle} \\ &\quad\times\left(\frac{\langle a, i+1\rangle}{\langle i+1, \lambda\rangle} - \frac{\langle a, i\rangle}{\langle i, \lambda\rangle}\right), \end{aligned} \tag{3.16}$$

[4]In fact, this is not as much of an abuse as it may seem. Note that evaluating the pole at $z\to\infty$ is equivalent to evaluating the pole at the origin minus the poles at finite z. The former would be a true collinear pole, while the latter would be a collinear pole with shifted l_1.

where the two equivalent representations focus on different adjacent collinear poles in the parentheses. The representation in Eq. (3.16) allows us to compute the bubble coefficient in a manner that manifests the relation between collinear poles in adjacent channels. With auxiliary spinor $|\alpha\rangle$ in Eq. (3.14) chosen to be $|a\rangle$, the bubble coefficient is

$$C^{(i,j)}_{2\{a,b\}} = C^{(i,j)}_{2\{a,b\}}(\lambda \sim j+1) + C^{(i,j)}_{2\{a,b\}}(\lambda \sim j) + C^{(i,j)}_{2\{a,b\}}(\lambda \sim i+1) + C^{(i,j)}_{2\{a,b\}}(\lambda \sim i).$$

Here we have used $(\lambda \sim j)$ to indicate the contribution from the collinear pole $\langle \lambda, j\rangle$. For convenience, we will refer to $(\lambda \sim j)$ and $(\lambda \sim j+1)$ collinear poles as "j-channel poles," and $(\lambda \sim i)$ and $(\lambda \sim i+1)$ poles as "i-channel poles." A graphical illustration of Eq. (3.18) is given in Fig. 10

Before proceeding, we point out a very important observation. Comparing the first line of Eq. (3.16) for $\hat{\mathcal{S}}^{(i,j)}_{\{a,b\},\mathcal{N}}|_{\mathcal{O}(z^0)}$ with that for $\hat{\mathcal{S}}^{(i,j-1)}_{\{a,b\},\mathcal{N}}|_{\mathcal{O}(z^0)}$,

$$\hat{\mathcal{S}}^{(i,j-1)}_{a,b}|_{\mathcal{O}(z^0)} = (\mathcal{N}-4)\mathcal{A}^{\text{tree}}_n \frac{\langle a,\lambda\rangle\langle b,\lambda\rangle^2\langle i,i+1\rangle}{\langle a,b\rangle^2\langle i,\lambda\rangle\langle i+1,\lambda\rangle} \times\left(\frac{\langle a,j\rangle}{\langle j,\lambda\rangle} - \frac{\langle a,j-1\rangle}{\langle j-1,\lambda\rangle}\right),$$

we immediately see that terms containing the common collinear pole of the two adjacent cuts, i.e., $1/\langle j,\lambda\rangle$, are exactly the same but crucially have opposite signs. This applies to all of the other terms in Eq. (3.16): each residue in the sum has a counterpart in the adjacent channel, as illustrated in Fig. 1.

At this point, one is tempted to conclude that the contribution to the bubble coefficient from common collinear channels cancels. However there is one subtlety. In Eq. (3.14), besides $\hat{\mathcal{S}}^{(i,j)}_{\{a,b\},\mathcal{N}}|_{\mathcal{O}(z^0)}$, there is an extra factor in the total derivative that depends on the total momentum of the two-particle cut, $P_{i+1,j}$, which will be distinct for the adjacent cuts. Luckily these distinct factors become identical on the common collinear pole:

$$\frac{[\tilde{\lambda}|P_{i+1,j}|a\rangle}{\langle\lambda|P_{i+1,j}|\tilde{\lambda}]\langle\lambda,a\rangle}\Bigg|_{\langle\lambda,j\rangle=[\tilde{\lambda},j]=0} = \frac{[\tilde{\lambda}|P_{i+1,j-1}|a\rangle}{\langle\lambda|P_{i+1,j-1}|\tilde{\lambda}]\langle\lambda,a\rangle}\Bigg|_{\langle\lambda,j\rangle=[\tilde{\lambda},j]=0}, \tag{3.17}$$

where $|_{\langle\lambda,j\rangle=[\tilde{\lambda},j]=0}$ indicates that the loop momentum is evaluated in the limit where it is collinear with j.[5] Because the extra factors are identical on the CCP, we now conclude that the contribution of the CCP to the bubble coefficient indeed cancels between adjacent channels. This can also be concretely checked against the result from the direct evaluation of the dLIPS integral:[6]

$$C^{(i,j-1)}_{2\{a,b\}}(\lambda\sim j) = -(\mathcal{N}-4)\mathcal{A}^{\text{tree}}_n \frac{\langle i,i+1\rangle}{\langle a,b\rangle^2} \times\frac{\langle a|P_{i+1,j-1}|j]}{\langle j+1|P_{i+1,j-1}|j]}\frac{\langle a,j\rangle\langle b,j\rangle^2}{\langle i,j\rangle\langle i+1,j\rangle},$$

$$C^{(i,j)}_{2\{a,b\}}(\lambda\sim j) = (\mathcal{N}-4)\mathcal{A}^{\text{tree}}_n \frac{\langle i,i+1\rangle}{\langle a,b\rangle^2}\frac{\langle a|P_{i+1,j}|j]}{\langle j|P_{i+1,j}|j]} \times\frac{\langle a,j\rangle\langle b,j\rangle^2}{\langle i,j\rangle\langle i+1,j\rangle}.$$

Adding these two equations, we find

$$C^{(i,j)}_{2\{a,b\}}(\lambda\sim j) + C^{(i,j-1)}_{2\{a,b\}}(\lambda\sim j) = (4-\mathcal{N})\mathcal{A}^{\text{tree}}_n \frac{\langle i,i+1\rangle}{\langle a,b\rangle^2}\frac{\langle a,j\rangle\langle b,j\rangle^2}{\langle i,j\rangle\langle i+1,j\rangle} \times\left[-\frac{\langle a|P_{i+1,j}|j]}{\langle j|P_{i+1,j}|j]} + \frac{\langle a|P_{i+1,j-1}|j]}{\langle j|P_{i+1,j-1}|j]}\right] = 0, \tag{3.18}$$

thus verifying our claim.

Since the four collinear poles for a generic two-particle cut are shared by four different adjacent channels as shown in Fig. 1, this immediately leads to the result that although the bubble coefficient for a generic two-particle cut is given by complicated rational functions, as shown in Eq. (3.18), in summing over all two-particle cuts there is a pairwise cancellation of CCP, and thus a majority of bubble coefficients do not contribute to the final result.

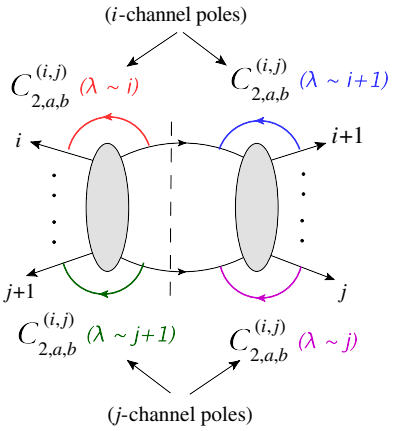

FIG. 10 (color online). A graphical representation of Eq. (3.18). The bubble coefficient of a given channel is separated into four terms, each having a different collinear pole as the origin of the holomorphic anomaly that gives a nonzero dLIPS integral. The four-contributions can be grouped into two channels: the i channel and the j channel.

[5]Since the contour of the dLIPS integral is taken to be real, $\tilde{\lambda} = \bar{\lambda}$, the collinear pole $1/\langle\lambda, j\rangle$ freezes the loop momenta to satisfy $\langle\lambda, j\rangle = [\tilde{\lambda}, j] = 0$.

[6]Explicit evaluation of this integral via the holomorphic anomaly [8,9,13] is reviewed in Appendix A.

The cancellation of CCP in adjacent channels leads to systematic cancellation in the sum of bubble coefficients and the sum telescopes. However, there are "terminal cuts" which contain unique poles that are not canceled. Below, we demonstrate that these so-called "terminal poles" constitute the sole contribution to the overall bubble coefficient. First we focus on the simplest case, namely the two external "negative-helicity" Ψ lines a, b are adjacent. The general case is treated in Sec. III B 2.

1. Adjacent MHV amplitudes

We consider split-helicity MHV amplitudes where the Ψ lines a, b are adjacent, i.e., $b = a - 1$. The systematic cancellation is illustrated in Fig. 11, where the dashed lines indicate pairs of CCP that cancel in the sum. Note that there are no contributions from the collinear poles where the loop leg is collinear with the Ψ lines, a and $a - 1$. This is because the residues of such poles are zero, as can be seen in Eq. (3.16) and explicitly checked in Eq. (3.18). One immediately sees that the summation is reduced to the two terminal poles. These are identified as poles in two-particle cuts with a 4-point tree amplitude on one side (and an n-point tree on the other), where the two loop momenta become collinear with the two external legs of the 4-point tree amplitude. A straightforward evaluation of the contribution of these two terminal poles yields the result for the sum of all bubble coefficients:

$$\begin{aligned}\mathcal{C}_{2\{a,a-1\}} &= C^{(a-3,a-1)}_{2\{a,a-1\}}(\lambda \sim a-2) + C^{(a+1,a-1)}_{2\{a,a-1\}}(\lambda \sim a+1) \\ &= -(\mathcal{N}-4)\mathcal{A}^{\text{tree}}_n + 0 = -\beta_0 \mathcal{A}^{\text{tree}}_n, \end{aligned} \tag{3.19}$$

with $\beta_0 = (\mathcal{N} - 4)$. Note that $C^{(a+1,a-1)}_{2\{a,a-1\}}(\lambda \sim a + 1) = 0$ is a result of our choice of reference spinor $|\alpha\rangle = |a\rangle$ in deriving Eq. (3.18). Were we to make the other natural choice, $|\alpha\rangle = |b\rangle = |a - 1\rangle$, we would instead have $C^{(a-3,a-1)}_{2\{a,a-1\}}(\lambda \sim a - 2) = 0$ and $C^{(a+1,a-1)}_{2\{a,a-1\}}(\lambda \sim a + 1) = -\beta_0 \mathcal{A}^{\text{tree}}_n$.

For example, take the 6-point MHV amplitude with legs 1 and 6 to be negative-helicity lines. The sum of bubble coefficients is given as

$$\begin{aligned}\mathcal{C}_{2\{1,6\}} &= C^{(2,6)}_{2\{1,6\}}(\lambda \sim 2) + C^{(2,6)}_{2\{1,6\}}(\lambda \sim 3) + C^{(3,6)}_{2\{1,6\}}(\lambda \sim 3) \\ &\quad + C^{(3,6)}_{2\{1,6\}}(\lambda \sim 4) + C^{(4,6)}_{2\{1,6\}}(\lambda \sim 4) + C^{(4,6)}_{2\{1,6\}}(\lambda \sim 5) \\ &= C^{(2,6)}_{2\{1,6\}}(\lambda \sim 2) + C^{(4,6)}_{2\{1,6\}}(\lambda \sim 5) = -\beta_0 \mathcal{A}^{\text{tree}}_n. \end{aligned} \tag{3.20}$$

We see that there are two pairs of common collinear poles, $\lambda \sim 3$ and $\lambda \sim 4$. The pairs cancel each other in the sum and one arrives at the two terminal pole which evaluates to the desired result. The cancellation is illustrated in Fig. 12.

Thus we have demonstrated that one of the terminal poles vanishes and the sum of bubble coefficients for adjacent MHV amplitudes for arbitrary n are given by a single terminal pole.

2. Nonadjacent MHV amplitudes

The above case with the two Ψ lines a, b being adjacent is simple because the j-channel poles [see below (3.16)] were absent. For MHV amplitudes with a, b being nonadjacent, the j-channel poles are now nonzero, and all the four collinear poles contribute in Eq. (3.18). The sum of bubble coefficients can be conveniently separated into a summation of the i-channel poles, and a summation of the j-channel poles. Cancellation of CCP in both channels again reduces the summation to the terminal poles. For simplicity, we set $a = 1$ and $1 < b$. We denote the terminal cut in the summation of i-channel poles by i_t, j, and similarly for the terminal cut of the j-channel poles by

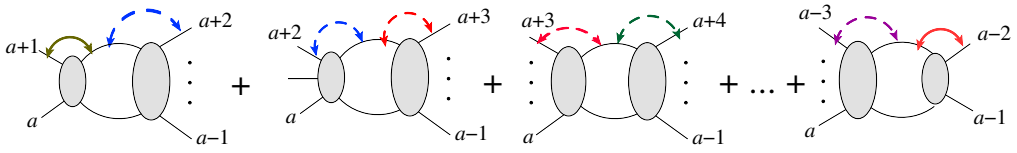

FIG. 11 (color online). A schematic representation of the cancellation of CCP for adjacent MHV amplitude for SYM. Each colored arrow represents a collinear pole that contributes to the bubble coefficient. Pairs of dashed arrows in the same color cancel. Only those represented by the solid arrows one on the two ends remain; they are the only nontrivial contribution to the overall bubble coefficient.

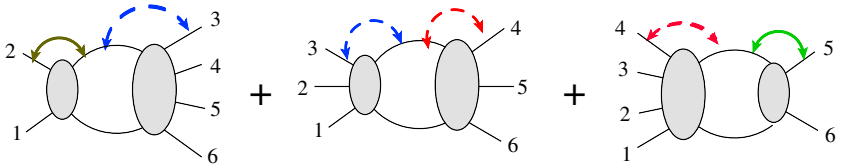

FIG. 12 (color online). A schematic representation of the cancellation of CCP for adjacent 6-point MHV amplitude. The dashed lines are common collinear poles, which cancel pairwise.

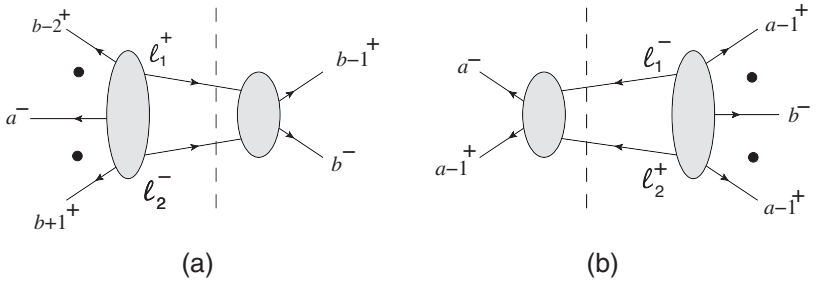

FIG. 13. The two terminal cuts for a given helicity configuration for the loop legs. For the choice of reference spinor $|\alpha\rangle = |a\rangle$ only diagram (a) is nonvanishing. If one instead chooses $|\alpha\rangle = |b\rangle$, then it is diagram (b) that gives the nontrivial contribution.

i, j_t. The contribution of these uncanceled poles are identified as

(i) i channel:

$$C^{(i_t,j)}_{2\{1,b\}}(\lambda \sim i_t) \quad \begin{matrix} \text{for } j = n, & i_t = 2 \\ \text{for } b \le j < n, & i_t = 1 \end{matrix},$$

$$C^{(i_t,j)}_{2\{1,b\}}(\lambda \sim i_t + 1) \quad \begin{matrix} \text{for } j = b, & i_t = b-2 \\ \text{for } b < j \le n, & i_t = b-1 \end{matrix},$$

(ii) j channel:

$$C^{(i,j_t)}_{2\{1,b\}}(\lambda \sim j_t) \quad \begin{matrix} \text{for } i = b-1, & j_t = b+1 \\ \text{for } 1 \le i < b-1, & j_t = b \end{matrix},$$

$$C^{(i,j_t)}_{2\{1,b\}}(\lambda \sim j_t + 1) \quad \begin{matrix} \text{for } i = 1, & i_t = n-1 \\ \text{for } 1 < i \le n-1, & j_t = n \end{matrix}.$$

In identifying the terminal poles, one has to take into account that, when summing over the i-channel poles, the value of j affects the possible values that i can take (and vice versa for the summation of j-channel poles). For a detailed discussion of the above result, we refer the reader to Appendix B where we perform a similar analysis for nonadjacent MHV amplitudes in pure Yang-Mills. As discussed in Sec. III B 1, the collinear poles where the loop momenta become collinear with a Ψ line have vanishing residues. In the present context, this refers to $(\lambda \sim 1)$ and $(\lambda \sim b)$. Thus there are only four contributing terms in the sum of bubble coefficients

$$\mathcal{C}_{2\{1,b\}} = C^{(2,n)}_{2\{1,b\}}(\lambda \sim 2) + C^{(b-2,b)}_{2\{1,b\}}(\lambda \sim b-1) + C^{(b-1,b+1)}_{2\{1,b\}}(\lambda \sim b+1) + C^{(1,n-1)}_{2\{1,b\}}(\lambda \sim n). \tag{3.21}$$

Extracting the corresponding expressions from Eq. (3.18), one finds that the first and last terms vanish. This is again due to the choice of reference spinor $|\alpha\rangle = |a\rangle$.[7] Thus the only contributions to the sum of bubble coefficients come from $C^{(b-1,b+1)}_{2\{1,b\}}(\lambda \sim b+1)$ and $C^{(b-2,b)}_{2\{1,b\}}(\lambda \sim b-1)$, which sum to

$$\mathcal{C}_{2\{1,b\}} = C^{(b-1,b+1)}_{2\{1,b\}}(\lambda \sim b+1) + C^{(b-2,b)}_{2\{1,b\}}(\lambda \sim b-1) = (4-\mathcal{N})\mathcal{A}^{\text{tree}}_n \frac{\langle 1,b-1\rangle\langle b,b+1\rangle + \langle b-1,b\rangle\langle 1,b+1\rangle}{\langle b-1,b+1\rangle\langle 1,b\rangle}$$
$$= -(\mathcal{N}-4)\mathcal{A}^{\text{tree}}_n. \tag{3.22}$$

This agrees with Eq. (1.4) with $\beta_0 = (\mathcal{N}-4)$.

In conclusion, for both adjacent and nonadjacent MHV amplitudes in $\mathcal{N} = 1$, 2 super Yang-Mills theory, the cancellation of CCP in the sum of bubble coefficients implies that for n-point (non)adjacent MHV amplitudes, only (two) one term in the sum of bubble coefficients gives a nontrivial contribution $\beta_0 \mathcal{A}^{\text{tree}}_n$. Thus the on-shell formalism achieves Eq. (1.4) in a systematic and simple way.

C. MHV bubble coefficients for pure Yang-Mills

The observed structure of cancellations for $\mathcal{N} = 1$, 2 super Yang-Mills theory is present in pure Yang-Mills as well. However, it is more involved to derive this since the $\mathcal{O}(z^0)$ part of the BCFW-shifted two-particle cut contains higher-order collinear poles. Nevertheless, adjacent channels again share these higher-order CCP, and their contribution to the sum of bubble coefficient also cancels. The cancellation of CCP renders the summation down to the terminal poles, which evaluate to $11/6 A^{\text{tree}}_n$. We present the detailed derivation of this in Appendix B.

[7] If we were to use the other natural choice, $|\alpha\rangle = |b\rangle$, we would arrive at the result that the second and third terms of Eq. (3.21) vanish. This apparent dependence of a particular double cut on the reference spinor is illusory: with care, one can cancel the full $|\alpha\rangle$ dependence from each individual bubble coefficient. However, this cancellation comes at the expense of the manifest $a \leftrightarrow b$ symmetry present in the uncanceled form. This asymmetry causes one term to seemingly vanish while the other gives the full bubble coefficient.

Here we would like to give a brief discussion on the nature of the terminal poles in pure Yang-Mills theory.

As discussed above, the terminal cuts are those where there is a 4-point tree amplitude on one side of the two-particle cut. The uncanceled terminal poles can be identified as the poles that arise when the loop momenta become collinear with the pair of external legs of this 4-point tree amplitude. For pure Yang-Mills, summing over the internal helicity configurations *before* taking the dz and dLIPS integrals obscures the nature of the cancellation.

Additional structure reveals itself if we *first* evaluate the contributions to the bubble coefficient for a given set of internal states, aka gluon helicity configuration, and *then* sum over internal states/helicities. Specifically, these double-forward terminal poles are nonzero only when the internal helicities of the loop legs leaving the n-point tree on one side of the cut match with the helicities of the pair of external lines in the 4-point tree on the other side of the cut (see Fig. 13). These "helicity-preserving" double poles (which will henceforth be called "double-forward poles") give the entire bubble coefficient.

Consider the internal helicity configuration (l_1^+, l_2^-) as shown in Figs. 8(b) and 13. There are two "helicity-preserving" terminal cuts: Figs. 13(a) and 13(b). Choosing the reference spinor $|\alpha\rangle = |a\rangle$, Fig. 13(b) vanishes, and Fig 13(a) evaluates to $11/6A_n^{\text{tree}}$, see Eq. (B25). If one were to make the other choice for the reference spinor, $|\alpha\rangle = |b\rangle$, we would instead have Fig. 13(a) vanishing, and Fig. 13(b) giving $11/6A_n^{\text{tree}}$. In fact, the helicity-preserving property of the contributing poles can also be seen for the $\mathcal{N} = 1, 2$ super Yang-Mills theory, where one simply substitutes the $+$ and $-$ helicity in the previous discussions with Ψ and Φ lines. This fact was obscured previously as the different internal multiplet configurations were summed to obtain the simple form of the two-particle cut in Eq. (3.13).

Thus we conclude that in the pure Yang-Mills theory the sum of bubble coefficients is simply given by the contribution of terminal poles where the helicity configuration is preserved, and where the loop momenta become collinear with the pair of external legs within the 4-point amplitude. For simplicity we will call these double-forward poles, due to the nature of the kinematics. In Sec. V we will show that for split-helicity N^{k}MHV bubble coefficients, these double-forward poles again produce the correct sum for the bubble coefficient, thus indicating complete cancellation among the remaining contributions. But before indulging in that story let us present a general argument for the cancellation of CCP.

IV. TOWARDS GENERAL CANCELLATION OF COMMON COLLINEAR POLES

In the above, we have shown that Eq. (1.4) can be largely attributed to the fact that the bubble coefficient for a given cut secretly shares the same terms with its four adjacent cuts, leading to systematic cancellations between them. We have proven this for n-point MHV amplitudes in both $\mathcal{N} = 1$, 2 super Yang-Mills as well as pure Yang-Mills theories (Appendix B). One can also consider adjoint scalars and fermions minimally coupled to gluons. Since at one loop, we can separate contributions from different spins inside the loop as

$$\begin{aligned}\text{fermions} &\to (\mathcal{N} = 1\,\text{SYM}) - (\text{YM})\\ \text{scalar} &\to (\mathcal{N} = 2\,\text{SYM}) - (\mathcal{N} = 1\,\text{SYM}) - (\text{fermions}),\end{aligned} \tag{4.1}$$

proof of cancellation of CCP for each of the theories (for MHV scattering) on the rhs of Eq. (4.1) implies that such cancellation occurs for each spin individually.

We would like to show this holds for N^{k}MHV amplitudes. Unfortunately, for N^{k}MHV amplitudes, multiparticle poles of tree amplitudes on either side of the cut contribute to the bubble coefficient, and the analysis becomes more complicated: cancellation of CCP is no longer sufficient to show terminal poles dominate the bubble coefficient. Nonetheless, we believe that the cancellation between CCP persists for arbitrary helicity configuration. As an indication, we demonstrate that the residues of CCP for adjacent cut always have the same form and opposite signs, for any helicity configuration.

Collinear limits of tree-level amplitudes in Yang-Mills theory, with $k_a = zk_P$, $k_b = (1-z)k_P$, factorize as

$$\begin{aligned}&A_n^{\text{tree}}(\ldots, a^{\lambda_a}, b^{\lambda_b}, \ldots)\\ &\quad\to \sum_{\lambda=\pm} \text{Split}_{-\lambda}^{\text{tree}}(z, a^{\lambda_a}, b^{\lambda_b}) A_{n-1}^{\text{tree}}(\ldots, P^{\lambda}, \ldots),\end{aligned} \tag{4.2}$$

where the factor $\text{Split}_{-\lambda}^{\text{tree}}(z, a^{\lambda_a}, b^{\lambda_b})$ is the gluon splitting amplitude. Its form for various helicity configurations are given by [15,19]

$$\begin{aligned}\text{Split}_{-}^{\text{tree}}(a^-, b^-) &= 0,\\ \text{Split}_{-}^{\text{tree}}(a^+, b^+) &= \frac{1}{\sqrt{z(1-z)}\langle ab\rangle},\\ \text{Split}_{+}^{\text{tree}}(a^+, b^-) &= \frac{(1-z)^2}{\sqrt{z(1-z)}\langle ab\rangle},\\ \text{Split}_{-}^{\text{tree}}(a^+, b^-) &= -\frac{z^2}{\sqrt{z(1-z)}[ab]}.\end{aligned} \tag{4.3}$$

Without loss of generality, we focus on the common collinear pole depicted in Fig. 5, in adjacent cuts $(1\ldots i-1|i\ldots n)$ and $(1\ldots i|i+1\ldots n)$. In other words, we study the collinear region with $l_1^{(i)} = \tau^{(i)}k_i$ and $l_1^{(i+1)} = \tau^{(i+1)}k_i$.[8] The two integrands become

[8]Strictly speaking, the condition $\langle l_1 i\rangle = 0$ only requires $\lambda_{l_1} \sim \lambda_i$. However since the dLIPS integration contour is along $\tilde{\lambda} = \bar{\lambda}$, the condition is equivalent to $l_1 \sim k_i$.

$$\begin{aligned}&\mathrm{Cut}_{(1..i-1|i..n)}|_{\langle l_1 i\rangle}\\&\quad= A_{i+1}(1,\ldots,i-1,\tau^{(i)}i,l_2^{(i)})\sum_{\lambda=\pm}\mathrm{Split}^{\mathrm{tree}}_{-\lambda}\\&\qquad\times A_{n-i+2}(-l_2^{(i)},(1-\tau^{(i)})i,i+1,\ldots,n),\end{aligned}\tag{4.4}$$

for cut $(1\ldots i-1|i\ldots n)$, and

$$\begin{aligned}&\mathrm{Cut}_{(1\ldots i|i+1\ldots n)}|_{\langle l_1 i\rangle}\\&\quad=\sum_{\lambda=\pm}\mathrm{Split}^{\mathrm{tree}}_{-\lambda}A_{i+1}(1,\ldots,(1+\tau^{(i+1)})i,l_2^{(i+1)})\\&\qquad\times A_{n-i+2}(-l_2^{(i+1)},-\tau^{(i+1)}i,i+1,\ldots,n),\end{aligned}\tag{4.5}$$

for cut $(1\ldots i|i+1\ldots n)$. The parameter $\tau^{(i)}$ can be fixed by the on-shell condition on $l_2^{(i)}$ since in the cut $(1\ldots i-1|i\ldots n)$, $l_2^{(i)}=P_{i-1}+\tau^{(i)}k_i$. Similar constraints from the cut $(1\ldots i|i+1\ldots n)$ fix $\tau^{(i+1)}$. This leads to

$$\begin{aligned}\tau^{(i)}&=\frac{P_{i-1}^2}{2k_i\cdot P_{i-1}}=\tau^{(i+1)}+1\longrightarrow l_2^{(i)}=P_{i-1}+\tau^{(i)}k_i\\&=P_i+\tau^{(i+1)}k_i=l_2^{(i+1)}.\end{aligned}$$

Substituting these results back into Eqs. (4.4) and (4.5), we see that the product of tree amplitudes is identical at their common collinear pole. Furthermore, by identifying the kinematic variables in the splitting amplitudes for each cut as

$$\begin{aligned}(1\ldots i-1|i\ldots n)\text{: }&k_a=k_i,k_b=-\tau^{(i)}k_i,z=\frac{1}{1-\tau^{(i)}}\\(1\ldots i|i+1\ldots n)\text{: }&k'_a=k_i,k'_b=\tau^{(i+1)}k_i,z'\\&=\frac{1}{1+\tau^{(i+1)}}=\frac{1}{\tau^{(i)}},\end{aligned}$$

we see that the splitting amplitudes for the two cuts are identical with a relative minus sign.[9]

The above analysis confirms that Eqs. (4.4) and (4.5) are indeed identical up to a minus sign. Thus the residue of the *entire two-particle cut* on the common collinear poles is identical and with opposite sign. This, however, does not directly lead to a proof of cancellation of CCP for bubble coefficients. This is because to extract the bubble coefficient, the two-particle cut must be translated into a total derivative in order for one to use holomorphic anomaly generated by the collinear poles to isolate the dLIPS integral. It is not guaranteed that after translating the two cuts into a total derivative form, the residues on the CCP will still be equal and opposite.

V. N^{k}MHV BUBBLE COEFFICIENTS

The cancellation of CCP, even if it holds for generic helicity configurations, is clearly not sufficient for simplifying the sum of bubble coefficients for N^{k}MHV amplitudes. The complications arise from the presence of multiparticle poles of the tree amplitudes in the two-particle cut. It is conceivable that there exists a similar cancellation of common multiparticle poles, since a trivial example would be the cancellation of CCP, considering the fact that collinear poles are secretly multiparticle poles via momentum conservation. Here we instead ask a more direct question: does the contribution of the double-forward poles to the bubble coefficient directly give $11/6A^{\mathrm{tree}}$ for n-point N^{k}MHV amplitude?

To facilitate our analysis, we will use the CSW representation [13,20,21] for the split-helicity NMHV tree amplitude $(---+\cdots+)$. We will show that at the double-forward poles, the contribution from each individual CSW diagram evaluates to $11/6$ times the original CSW diagram whose loop momenta are replaced by the corresponding external lines. Summing the different diagrams one simply recovers $11/6$ times the CSW representation of the tree amplitude. Using induction, we prove that this is still true for all n-point split-helicity N^{k}MHV amplitudes.

A. Double-forward poles in terminal cuts of $A_n^{\text{1-loop}}(---+\cdots+)$

The split-helicity configuration for NMHV amplitudes is the simplest to analyze. The CSW form for n-particle NMHV scattering, with adjacent negative-helicity gluons is given by the following $2(n-3)$ terms [13]:

$$\begin{aligned}&A(1^-,2^-,3^-,4^+,\ldots,n^+)\\&\quad=\sum_{i=4}^{n}\frac{\langle1,2\rangle^3}{\langle P_{3,i},i+1\rangle\cdots\langle P,2\rangle}\frac{1}{P_{3,i}^2}\frac{\langle P_{3,i},3\rangle^3}{\langle3,4\rangle\cdots\langle i,P_{3,i}\rangle}\\&\qquad+\sum_{i=4}^{n}\frac{\langle1,P_{2,i-1}\rangle^3}{\langle P_{2,i-1},i\rangle\cdots\langle n,1\rangle}\frac{1}{P_{2,i-1}^2}\\&\qquad\times\frac{\langle2,3\rangle^3}{\langle P_{2,i-1},2\rangle\cdots\langle i-1,P_{2,i-1}\rangle},\end{aligned}\tag{5.1}$$

where $|P_{i,j}\rangle\equiv P_{i,j}|\tilde\eta]$, and $\tilde\eta$ is an auxiliary spinor.

For helicity configuration (l_1^-,l_2^+), the terminal cuts are shown in Fig. 14. We first focus on cut (a), which is given by $A_4(\hat l_1^+,3^-,4^+,\hat l_2^-)\times A_n(\hat l_2^+,5^+,\ldots,n^+,\ldots,1^-,2^-,\hat l_1^-)$. Cut (b) in Fig. 14 evaluates in exactly the same way. We use the CSW expansion on the n-particle NMHV subamplitude as indicated in Fig. 15:

$$[\mathrm{cut}\,(a)]|_{df}=[\mathrm{diag}(a)+\mathrm{diag}(b)+\mathrm{diag}(c)]|_{df}.\tag{5.2}$$

Notice for Figs. 15(a) and 15(b), the loop legs are on the same MHV vertex and hence the CSW propagator $1/P^2$ does not depend on z. This implies that from the point of view of extracting the pole at $z\to\infty$ and performing the dLIPS integration, only the MHV vertex on which the loop legs are attached is relevant. Hence the evaluation of the double-forward poles is simply evaluating the contribution

[9]For consistency, we take the positive branch of the square root.

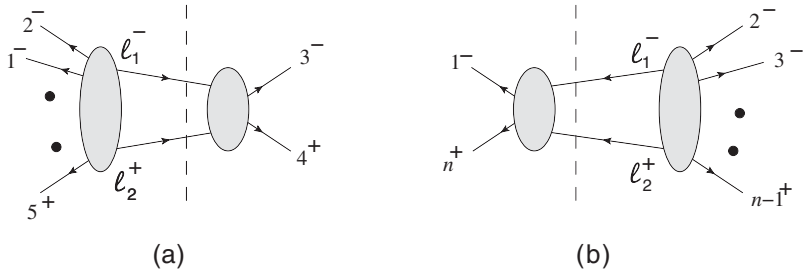

FIG. 14. The terminal cuts of the split-helicity NMHV amplitude that contain the two helicity-preserving double-forward poles.

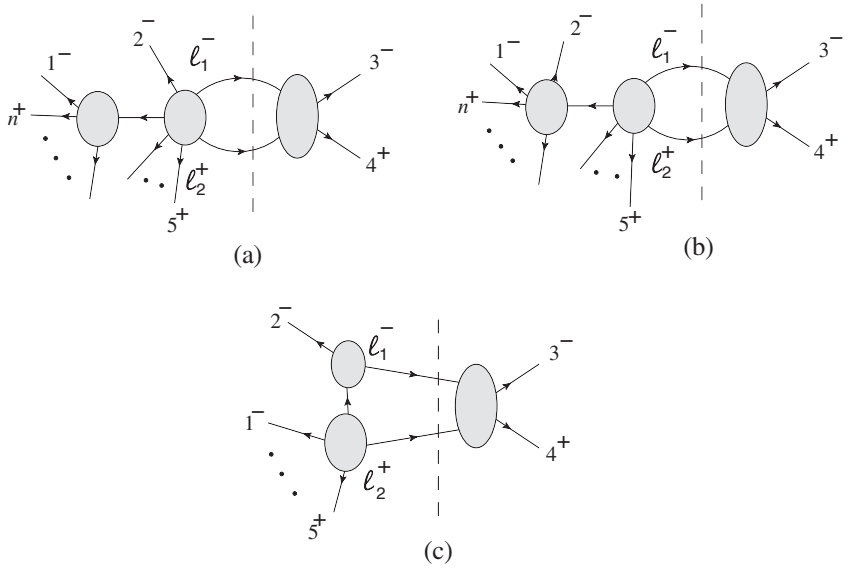

FIG. 15. Representing the tree amplitude in the terminal cuts with CSW expansion. Note that the loop legs are attached to the same MHV vertex for diagrams (a) and (b). The dLIPS integration for these diagrams is exactly the same as that computed for adjacent MHV bubbles.

of that for a MHV amplitude with one on-shell leg identified with CSW propagator leg multiplied by the remaining CSW vertices which behave as spectators to the dLIPS integration. This realization makes the computation trivial, as we know the double-forward pole contributes $11/6$ times the tree amplitude. This implies that here the result would simply be $11/6$ times the corresponding CSW tree diagram. One can thus straightforwardly obtain

$$\begin{aligned}&[\mathrm{diag}(a)+\mathrm{diag}(b)]|_{df}\\&=\frac{11}{6}\Bigg(\sum_{i=4}^{n}\frac{\langle 1,2\rangle^3}{\langle P_{3,i},i+1\rangle\cdots\langle P,2\rangle}\frac{1}{P_{3,i}^2}\frac{\langle P_{3,i},3\rangle^3}{\langle 3,4\rangle\cdots\langle i,P_{3,i}\rangle}\\&\quad+\sum_{i=5}^{n}\frac{\langle 1,P_{2,i-1}\rangle^3}{\langle P_{2,i-1},i\rangle\cdots\langle n,1\rangle}\frac{1}{P_{2,i-1}^2}\\&\quad\times\frac{\langle 2,3\rangle^3}{\langle P_{2,i-1},2\rangle\cdots\langle i-1,P_{2,i-1}\rangle}\Bigg),\end{aligned}\tag{5.3}$$

where $|_{df}$ indicates the contribution from the double-forward pole. There is another type of contribution, as shown in Fig. 15(c), where the CSW propagator depends on z and we need a careful analysis as follows.

Denoting $|\hat{P}\rangle=\hat{P}|\tilde{\eta}]$, which accounts for the z dependence of the CSW propagator, the cut integrand is given by

$$\begin{aligned}\mathrm{diag}(c)=&\frac{\langle 1,\hat{P}\rangle^3}{\langle\hat{P},l_2\rangle\langle\hat{l}_2,5\rangle\cdots\langle n,1\rangle}\frac{1}{\hat{P}^2}\frac{\langle 2,\hat{l}_1\rangle^3}{\langle\hat{P},2\rangle\langle\hat{l}_1,\hat{P}\rangle}\\&\times\frac{\langle 3,\hat{l}_2\rangle^4}{\langle 3,4\rangle\langle 4,l_2\rangle\langle l_2,\hat{l}_1\rangle\langle\hat{l}_1,3\rangle},\end{aligned}\tag{5.4}$$

where $\hat{P}=p_2+\hat{l}_1$. We call this the "hard" term. The other $2n-5$ terms we call the "easy" terms. For simplicity, we first strip off the corresponding tree factor, i.e., the $i=4$ term in the second line of Eq. (5.1),

$$T_{2,3}=\frac{\langle 1,P_{2,3}\rangle^3}{\langle P_{2,3},4\rangle\langle 4,5\rangle\cdots\langle n,1\rangle}\frac{1}{P_{2,3}^2}\frac{\langle 2,3\rangle^3}{\langle P_{2,3},2\rangle\langle 3,P_{2,3}\rangle}\tag{5.5}$$

from the terminal dLIPS integrand in Eq. (5.4). This yields

$$\mathrm{diag}(c) = T_{2,3}\Bigg(\frac{\langle 1,\hat{P}\rangle^3\langle P_{2,3},4\rangle\langle 4,5\rangle}{\langle 1,P_{2,3}\rangle^3\langle\hat{P},l_2\rangle\langle l_2,5\rangle}\frac{P_{2,3}^2}{\hat{P}^2}\frac{\langle 2,\hat{l}_1\rangle^3}{\langle\hat{P},2\rangle\langle\hat{l}_1,\hat{P}\rangle} \times \frac{\langle P_{2,3},2\rangle\langle 3,P_{2,3}\rangle\langle 3,l_2\rangle^4}{\langle 2,3\rangle^3\langle 3,4\rangle\langle 4,l_2\rangle\langle l_2,\hat{l}_1\rangle\langle\hat{l}_1,3\rangle}\Bigg). \tag{5.6}$$

We would like to put this into a form where we can readily take the large-z pole followed by the dLIPS integral about the double-forward pole. To simplify the analysis, we work out the explicit form of the spinor-inner products:

$$\begin{aligned}
|\hat{P}\rangle &= (p_2+\hat{l}_1)|\tilde{\eta}] \Rightarrow \{\langle\hat{l}_1,\hat{P}\rangle = \langle\hat{l}_1,2\rangle[2,\tilde{\eta}],\langle l_2,\hat{P}\rangle \\
&= \langle l_2,2\rangle[2,\tilde{\eta}] + \langle l_2,\hat{l}_1\rangle[l_1,\tilde{\eta}],\langle 2,\hat{P}\rangle \\
&= \langle 2,\hat{l}_1\rangle[l_1,\tilde{\eta}],\langle 1,\hat{P}\rangle = \langle 1,\hat{l}_1\rangle[l_1,\tilde{\eta}] + \langle 1,2\rangle[2,\tilde{\eta}]\}, \\
|P_{2,3}\rangle &= (p_2+p_3)|\tilde{\eta}] \Rightarrow \{\langle 3,P_{2,3}\rangle = \langle 3,2\rangle[2,\tilde{\eta}],\langle l_2,P_{2,3}\rangle \\
&= \langle l_2,2\rangle[2,\tilde{\eta}] + \langle l_2,3\rangle[3,\tilde{\eta}],\langle 2,P_{2,3}\rangle \\
&= \langle 2,3\rangle[3,\tilde{\eta}],\langle 1,P_{2,3}\rangle \\
&= \langle 1,3\rangle[3,\tilde{\eta}] + \langle 1,2\rangle[2,\tilde{\eta}]\}.
\end{aligned} \tag{5.7}$$

Applying Eq. (5.7) to Eq. (5.6), canceling all common factors, and setting $|\tilde{\eta}] = |2]$,[10] we find

$$\begin{aligned}
&\mathrm{diag}(c) \\
&= T_{2,3}\frac{\langle 1\hat{l}_1\rangle^3\langle 4,5\rangle\langle 3,l_2\rangle^4}{\langle 13\rangle^3\langle\hat{l}_1 l_2\rangle^2\langle l_2,5\rangle\langle 4,l_2\rangle\langle\hat{l}_1,3\rangle} \\
&= T_{2,3}\Bigg[\Bigg(\frac{\langle 3,4\rangle}{\langle l_2,4\rangle} - \frac{\langle 3,5\rangle}{\langle l_2,5\rangle}\Bigg)\frac{\langle\hat{l}_1,l_2\rangle}{\langle\hat{l}_1,3\rangle}\Bigg(-1+\frac{\langle 1,l_2\rangle\langle\hat{l}_1,3\rangle}{\langle 1,3\rangle\langle\hat{l}_1,l_2\rangle}\Bigg)^3\Bigg].
\end{aligned} \tag{5.8}$$

Expanding around $z\to\infty$, one finds

$$\begin{aligned}
\mathrm{diag}(c)|_{z\to\infty} = T_{2,3}\Bigg[&\Bigg(\frac{\langle 3,4\rangle}{\langle l_2,4\rangle} - \frac{\langle 3,5\rangle}{\langle l_2,5\rangle}\Bigg)\Bigg(3\frac{\langle 1,l_2\rangle}{\langle 1,3\rangle} \\
&- 3\frac{\langle 1,l_2\rangle^2\langle l_1,3\rangle}{\langle 1,3\rangle^2\langle l_1,l_2\rangle} + \frac{\langle 1,l_2\rangle^3\langle l_1,3\rangle^2}{\langle 1,3\rangle^3\langle l_1,l_2\rangle^2}\Bigg)\Bigg].
\end{aligned}$$

The double-forward pole corresponds to the $\langle l_2,4\rangle$ pole. A straightforward evaluation of the residue gives

$$\begin{aligned}
\mathrm{diag}(c)|_{df} &= T_{2,3}\int d\mathrm{LIPS}\frac{\langle 3,4\rangle}{\langle l_2,4\rangle}\Bigg(3\frac{\langle 1,l_2\rangle}{\langle 1,3\rangle} - 3\frac{\langle 1,l_2\rangle^2\langle l_1,3\rangle}{\langle 1,3\rangle^2\langle l_1,l_2\rangle} + \frac{\langle 1,l_2\rangle^3\langle l_1,3\rangle^2}{\langle 1,3\rangle^3\langle l_1,l_2\rangle^2}\Bigg) \\
&= \Bigg(3\times 1 - 3\times\frac{1}{2} + 1\times\frac{1}{3}\Bigg)T_{2,3} = \frac{11}{6}T_{2,3}.
\end{aligned}$$

In summary, we find that the double-forward pole of the terminal cuts sum to give

$$\begin{aligned}
[\mathrm{diag}(a)+\mathrm{diag}(b)+\mathrm{diag}(c)]|_{df} &= \frac{11}{6}\Bigg(\sum_{i=4}^{n}\frac{\langle 1,2\rangle^3}{\langle P_{3,i},i+1\rangle\cdots\langle P,2\rangle}\frac{1}{P_{3,i}^2}\frac{\langle P_{3,i},3\rangle^3}{\langle 3,4\rangle\cdots\langle i,P_{3,i}\rangle}\Bigg) \\
&+ \frac{11}{6}\Bigg(\sum_{i=5}^{n}\frac{\langle 1,P_{2,i-1}\rangle^3}{\langle P_{2,i-1},i\rangle\cdots\langle n,1\rangle}\frac{1}{P_{2,i-1}^2}\frac{\langle 2,3\rangle^3}{\langle P_{2,i-1},2\rangle\cdots\langle i-1,P_{2,i-1}\rangle}\Bigg) \\
&+ \frac{11}{6}\Bigg(\frac{\langle 1,P_{2,3}\rangle^3}{\langle P_{2,3},4\rangle\langle 4,5\rangle\cdots\langle n,1\rangle}\frac{1}{P_{2,3}^2}\frac{\langle 2,3\rangle^3}{\langle P_{2,3},2\rangle\langle 3,P_{2,3}\rangle}\Bigg) \\
&= \frac{11}{6}A(1^-,2^-,3^-,4^+,\ldots,n^+).
\end{aligned} \tag{5.9}$$

Thus indeed the double-forward limit of Fig. 14(a) gives the expected proportionality factor from the sum of bubble coefficients, suggesting complete cancellation of contributions from all the other channels and poles.

We see that using the CSW representation for NMHV tree amplitudes reveals the following structure: the double-forward poles in the terminal cut contribute a factor $11/6$ for *each* CSW tree diagram. Note that all but one term, Fig. 15(c), goes through trivially as the dLIPS only sees one MHV vertex in the NMHV tree amplitude. There is a more straightforward way of understanding the factor of $11/6$ in Fig. 15(c), which goes as follows.

Consider the same calculation for the split-helicity NMHV 5-point amplitude. Since this is secretly a 5-point $\overline{\mathrm{MHV}}$ amplitude we know that the forward poles for a given internal helicity configuration evaluate to $11/6\times\overline{\mathrm{MHV}}$, as proven previously. Now consider the same evaluation using the CSW representation. Since Figs. 15(a) and 15(b) automatically yield $11/6$ times the corresponding CSW tree diagram, Fig. 15(c) must give $11/6$ times its corresponding CSW tree diagram, $T_{2,3}$.

[10]This ordering of steps is important: this cancels an apparent factor of $[2,\tilde{\eta}]$ in the denominator of Eq. (5.6).

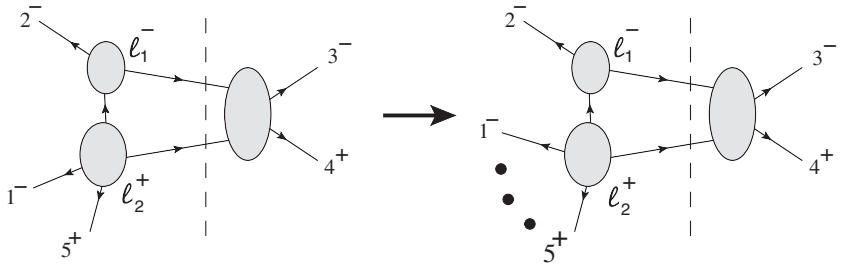

FIG. 16. Figure 15(c) for the 5-point amplitude. Going from 5-point to arbitrary n-point simply corresponds to adding additional plus helicity legs on the bottom MHV vertex. Since this modification affects neither extraction of constant term for $z \to \infty$ nor evaluation of the dLIPS integral, the $11/6$ factor obtained at 5-points holds for arbitrary n.

Now, for higher-point NMHV amplitudes, Fig. 15(c) is modified by additional plus helicity legs on one of the MHV vertices, as indicated in Fig. 16. From the point of view of expanding around the pole at $z \to \infty$ and the dLIPS integral, these additional plus helicity legs are simply spectators and do not participate. Thus the evaluation of Fig. 15(c) "must" be $11/6\ T_{2,3}$ as explicitly shown above. Note that this way of understanding the result of the double-forward poles allows us to generalize to N^{k}MHV.

B. Recursive generalization to N^{k}MHV bubble coefficients

We are now ready to give inductive proof that the residue at the double-forward poles gives the entire bubble coefficient, $11/3 \times A_n^{\text{tree}}$, for general split-helicity N^{k}MHV amplitudes. The proof is as follows.

(i) Using the CSW representation of N^{k}MHV amplitude, the diagrams that appear inside the terminal cut can be categorized by the number of z-dependence CSW propagators. For a given k there will be at most k propagators that have nontrivial z dependence. Diagrams that have $p < k$, z-dependent CSW propagators will be diagrams that have already appeared in the analysis for N^{p}MHV amplitudes, hence are known to give $11/6$ times the corresponding CSW tree diagram.

(ii) There will be a unique diagram that has k, z-dependent, CSW propagators. To evaluate this diagram, we note that the $k+4$-point split-helicity N^{k}MHV amplitude is the same as a $k+4$-point adjacent $\overline{\text{MHV}}$ amplitude, for which we know that the forward limit poles give $11/6 A_n^{\text{tree}}$. In the CSW representation, since all other diagrams already evaluate to $11/6$ times the corresponding tree diagram, as discussed in the previous step, this final diagram must as well.

(iii) For arbitrary n, one simply adds additional positive-helicity legs to MHV vertices. These extra states do not participate in the expansion around the pole at $z \to \infty$ or in the dLIPS integral. The modification only appears as an overall factor, and thus proves that for general n this last diagram also evaluates to $11/6$ times the corresponding CSW tree diagram.

(iv) Summing all the CSW diagrams in the double cut, we obtain $11/6 \times A_n^{\text{tree}}$ for the forward pole contribution to the bubble coefficient from the terminal cut.

(v) The other internal helicity configuration evaluates in the same way, on the other helicity-preserving double-forward terminal pole, yielding $\mathcal{C}_2 = 11/3 \times A_n^{\text{tree}}$

We use the N^{2}MHV amplitude to illustrate the above steps. The CSW representation for the N^{2}MHV terminal cut is given in Fig. 17. Figures 17(a) and 17(b) have no z-dependent CSW propagators, and hence from the point of view of extracting the constant piece at $z \to \infty$ and integrating over dLIPS, the two leftmost MHV vertices

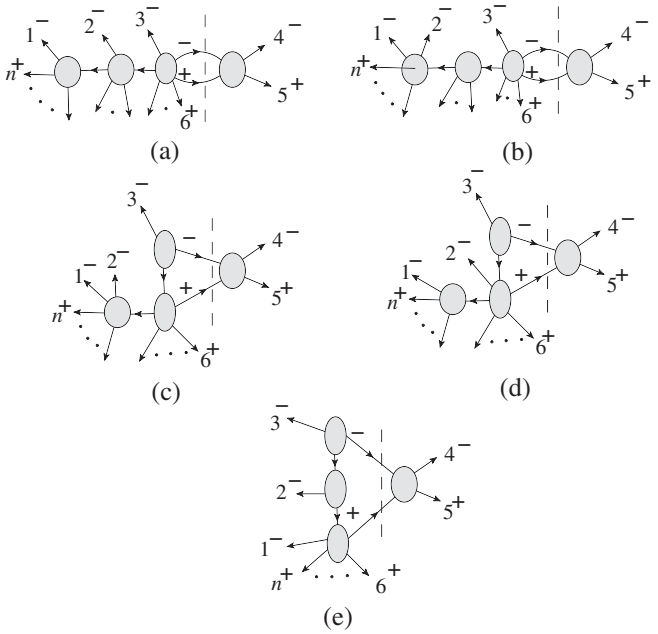

FIG. 17. The CSW representation of the terminal cut for N^{2}MHV amplitude. The evaluation of diagrams (a) and (b) is identical to that of adjacent MHV amplitudes, while the evaluation of diagrams (c) and (d) is identical to split-helicity NMHV amplitude.

are just spectators and the evaluation is on the rightmost MHV vertex on the left-hand side of the cut. Thus the evaluation of Figs. 17(a) and 17(b) is identical to the evaluation of the adjacent MHV amplitudes. For Figs. 17(c) and 17(d), there is one z-dependent CSW propagator. The MHV vertex where 1^- sits is again a spectator and the evaluation is identical to that of Fig. 15(c) for the NMHV amplitude, and hence evaluates to $11/6$ times the corresponding CSW tree diagram. Finally, for the unique Fig. 17(e), we use the argument that for $n = 6$, this is simply the $\overline{\text{MHV}}$ amplitude, from which we deduce that this term must also evaluate to $11/6$ times the corresponding tree diagram. This result will not be modified for $n > 6$, and hence completes the proof.

VI. CONCLUSION AND FUTURE DIRECTIONS

In this paper, we study the proportionality between the sum of bubble coefficients and the tree amplitude, which is required for renormalizability. For theories where Feynman diagram analysis is tractable, such as scalar theory and pure scalar amplitudes of Yukawa theory, we find that the bubble coefficient only receives contributions from a small class of one-loop diagrams. The contribution of each diagram is proportional to a tree diagram, and hence summing over all one-loop diagrams that give nontrivial contributions is equivalent to summing over tree diagrams. Crucially, these *new* tree diagrams are not necessarily present in the original tree amplitude of the theory. Through restricting our attention to theories where these new tree structures match those in the original tree amplitude, we accurately reproduce the known renormalization conditions derived from power counting analysis.

For (super)Yang-Mills theory, we show that the bubble coefficient for MHV amplitudes can be organized in terms of their origin as collinear poles, which are responsible for the nontrivial contribution to the dLIPS integration in the two-particle cuts. This representation reveals the existence of systematic cancellation in the sum of bubble coefficient. In particular, the residues of CCP cancel, and the sum telescopes down to unique terminal poles. These are poles that arise from cuts that have at least a 4-point tree amplitude on one side of the cut, and the helicity configuration of the internal legs must match that of the two external legs on the 4-point tree amplitude, as shown in Fig. 2. We conjecture that these double-forward poles are the only nontrivial contribution to the sum of bubble coefficients for any helicity configuration. As further evidence, we explicitly prove that for split-helicity n-point N^{k}MHV amplitudes, the contribution of each terminal pole indeed gives $11/6$ times the tree amplitude.

For more generic external helicity configurations, it will be interesting to see how the contributions from the multiparticle poles cancel with each other. An even more interesting example would be gravity. It is well known that pure gravity is one-loop finite [22]. The bubble coefficient is nonvanishing for generic two-particle cuts, and hence massive cancellation must occur. The lack of color ordering for gravity amplitudes indicates the pole structure that gives rise to the nontrivial contributions for the dLIPS integral is more complicated than Yang-Mills: presumably new cancellation mechanisms are required even for MHV amplitudes.

We demonstrate that the UV divergence of the one-loop gauge theory amplitude is completely captured by the residues of a set of unique collinear poles, i.e., it is controlled by a residue at finite loop momentum value. If the same holds for gravity, then through KLT relations [23] the residue of gravity is intimately tied to gauge theories, and it will be interesting to see how the relationship allows cancellation among terminal residues, leading to the known finiteness result for gravity and its relationship to BCJ duality [24,25]. Note that the study of tensor bubbles has previously revealed improved UV behavior for gravity amplitudes compared to naive power counting from Einstein-Hilbert action [26]. Even though it is well known that gravity is finite at one loop, a careful analysis of how finiteness is achieved for generic amplitudes may shed light on additional structure, as we have successfully achieved for (super) Yang-Mills amplitudes.

ACKNOWLEDGMENTS

We thank Nima Arkani-Hamed, Simon Caron-Huot, and Michael Kiermaier for many enlightening discussions. We are especially grateful to Zvi Bern, Lance Dixon, and Henriette Elvang for careful reading of our draft and giving us helpful suggestions. Y. H. is grateful for the Institute of Advanced Study for an invitation as a visiting member. Y. H. would also like to thank the Isaac Newton Institute for Mathematical Sciences for organizing the workshop "Recent Advances in Scattering Amplitudes," during which part of this work was completed. Y. H. was supported by the U.S. Department of Energy under Award No. DE–FG03–91ER40662. D. A. M. is supported NSF GRFP Grants No. DGE-1148900 and No. PHY-0756966. C. P. is supported by NSF Grant No. PHY-0953232, and in part by the DOE Award No. DE-FG02-95ER 40899.

APPENDIX A: dLIPS INTEGRALS VIA THE HOLOMORPHIC ANOMALY IN FOUR DIMENSIONS

Following Refs. [8,9,13], we can calculate integrals of the following form:

$$\oint_{\tilde{\lambda}=\bar{\lambda}} P^2 \frac{\langle \lambda, d\lambda\rangle[\tilde{\lambda}, d\tilde{\lambda}]}{\langle \lambda|P|\tilde{\lambda}]^2} \frac{\prod_{i=1}^{n}[a_i, \tilde{\lambda}]}{\langle \lambda|P|\tilde{\lambda}]^n} g(\lambda), \quad \text{where}$$
$$g(\lambda) = \frac{\prod_{j=1}^{m}\langle b_j, \lambda\rangle}{\prod_{k=1}^{m}\langle c_k, \lambda\rangle}, \tag{A1}$$

where the integral over phase space (dLIPS integral) is really a contour integral over two complex numbers. Two cases are important here: $n = 0$ for scalar and Yukawa theory, and $n = 2$ for gauge theories. Note:

$$P^2\frac{[\tilde{\lambda}, d\tilde{\lambda}]}{\langle\lambda|P|\tilde{\lambda}]^2} = -d\tilde{\lambda}^{\dot{\alpha}}\frac{\partial}{\partial\tilde{\lambda}^{\dot{\alpha}}}\left(\frac{[\tilde{\lambda}, \tilde{\eta}]P^2}{\langle\lambda|P|\tilde{\lambda}]\langle\lambda|P|\tilde{\eta}]}\right) = -d\tilde{\lambda}^{\dot{\alpha}}\frac{\partial}{\partial\tilde{\lambda}^{\dot{\alpha}}}\left(\frac{[\tilde{\lambda}|P|\alpha\rangle}{\langle\lambda|P|\tilde{\lambda}]\langle\lambda, \alpha\rangle}\right), \tag{A2}$$

where we have introduced reference spinors $|\tilde{\eta}] = P|\alpha\rangle$ in order to express the dLIPS integration measure as a total derivative. We further note that integrands of the form (A1) can be reduced to this basic measure through repeated differentiation. Concretely, for $n = 2$:

$$\frac{[I, \tilde{\lambda}][J, \tilde{\lambda}]}{\langle\lambda|P|\tilde{\lambda}]^4} = \frac{1}{6}\tilde{I}^{\dot{\gamma}}\tilde{J}^{\dot{\beta}}\frac{\partial^2}{\partial(\langle\lambda|P)^{\dot{\beta}}\partial(\langle\lambda|P)^{\dot{\gamma}}}\left\{\frac{1}{\langle\lambda|P|\tilde{\lambda}]^2}\right\}. \tag{A3}$$

For the case of MHV bubble integrands, the only reference spinors are of the form $|I] = P|i\rangle$. Combining (A2) and (A3), and interchanging the order of differentiation, one can rewrite the "$n = 2$" integrand as a total derivative:

$$\begin{aligned}\oint_{\tilde{\lambda}=\bar{\lambda}} P^2\frac{\langle\lambda, d\lambda\rangle[\tilde{\lambda}, d\tilde{\lambda}]}{\langle\lambda|P|\tilde{\lambda}]^4}\langle i|P|\tilde{\lambda}]\langle j|P|\tilde{\lambda}]g(\lambda) &= \oint_{\tilde{\lambda}=\bar{\lambda}}\langle\lambda, d\lambda\rangle\Bigg(-d\tilde{\lambda}^{\dot{\gamma}}\frac{\partial}{\partial\tilde{\lambda}^{\dot{\gamma}}}\Bigg[\frac{[\tilde{\lambda}|P|\alpha\rangle g(\lambda)}{\langle\lambda|P|\tilde{\lambda}]\langle\lambda, \alpha\rangle}\frac{1}{3}\\ &\times\left\{\frac{\langle i|P|\tilde{\lambda}]\langle j|P|\tilde{\lambda}]}{\langle\lambda|P|\tilde{\lambda}]^2} + \frac{\langle i, \alpha\rangle\langle j, \alpha\rangle}{\langle\lambda, \alpha\rangle^2}\right.\\ &\left.+\frac{1}{2}\frac{\langle i|P|\tilde{\lambda}]\langle j, \alpha\rangle + \langle i, \alpha\rangle\langle j|P|\tilde{\lambda}]}{\langle\lambda|P|\tilde{\lambda}]\langle\lambda, \alpha\rangle}\right\}\Bigg]\Bigg).\end{aligned} \tag{A4}$$

The last form for the integrand rewritten as a total derivative vanishes at all points save when it hits a simple pole. This is because along the integration contour $\tilde{\lambda} = \bar{\lambda}$, one has [13]

$$-d\tilde{\lambda}^{\dot{\alpha}}\frac{\partial}{\partial\tilde{\lambda}^{\dot{\alpha}}}\frac{1}{\langle\lambda, \xi\rangle} = -2\pi\bar{\delta}(\langle\lambda, \xi\rangle), \tag{A5}$$

$$\int\langle\lambda d\lambda\rangle\bar{\delta}(\langle\lambda, \xi\rangle)B(\lambda) = iB(\xi). \tag{A6}$$

Thus the dLIPS integral is localized to the poles $1/\langle\lambda, \xi\rangle$ of the integrand.[11] Each term in the integrand (A4) has potential collinear divergences coming from the spinor brackets in the denominator of $g(\lambda)$ and that of the reference spinor $\langle\lambda, \alpha\rangle \to 0$.

Through (A2) and (A5), we see that the simple bubble integrals in scalar QFT in Sec. II simply evaluate to $\int d\text{LIPS}(1) = -2\pi i$. For MHV bubble integrands, such as Eq. (3.16), there is always a choice of the reference spinor, such as $|\alpha\rangle = |a\rangle$, which eliminates the unphysical $1/\langle\lambda, \alpha\rangle$ pole.

[11]Note that $1/\langle\lambda|P|\tilde{\lambda}]$ is not a simple pole on the contour $\tilde{\lambda} = \bar{\lambda}$.

APPENDIX B: SUM OF MHV BUBBLE COEFFICIENTS FOR PURE YANG-MILLS

As mentioned in Sec. III C, the observed structure of cancellations for $\mathcal{N} = 1$, 2 super Yang-Mills theory is present in pure Yang-Mills as well. However, it is more involved to derive this since the $\mathcal{O}(z^0)$ part of the BCFW-shifted two-particle cut contains higher-order collinear poles. Nevertheless, adjacent channels again share these higher-order CCP, and their contribution to the sum of bubble coefficient also cancels. The cancellation of CCP renders the summation down to the terminal poles, which evaluate to $11/6A_n^{\text{tree}}$. Here, we explicitly deal with the details of this computation.

We begin with a generic BCFW-shifted two-particle cut of $(j+1, \ldots, a, \ldots, i|i+1, \ldots, b, \ldots, j)$ for nonadjacent MHV amplitude $A_n^{\text{MHV}}(a^-, b^-)$. Choosing the helicity configuration for the internal lines to be (l_1^+, l_2^-) on the lhs of the cut, as shown in Fig. 18, one has

$$\begin{aligned}S_{a,b}^{(i,j)} = A_n^{\text{tree}}&\left\{\frac{\langle i, i+1\rangle\langle b, \hat{l}_1\rangle}{\langle i, \hat{l}_1\rangle\langle\hat{l}_1, i+1\rangle}\right\}\left\{\frac{\langle j, j+1\rangle\langle a, l_2\rangle}{\langle j, l_2\rangle\langle l_2, j+1\rangle}\right\}\frac{\langle l_2, l_1\rangle}{\langle a, b\rangle}\\ &\times\left(\frac{\langle a, l_2\rangle\langle b, \hat{l}_1\rangle}{\langle a, b\rangle\langle l_1, l_2\rangle}\right)^3.\end{aligned} \tag{B1}$$

Let us extract the bubble coefficient by shifting the loop legs as $|\hat{l}_1\rangle \to |l_1\rangle + z|l_2\rangle$. Note that for our choice of shift, it will be convenient to take $|l_2\rangle = |\lambda\rangle$ as the dLIPS integration spinor. Under the dLIPS integration, there are three kinds of poles that would contribute to the holomorphic anomaly: (1) the $1/\langle\lambda\alpha\rangle$ poles that arise from writing the dLIPS integral as a total derivative, (2) the collinear poles of the form $1/\langle l_2 i\rangle$, and (3) the poles that come from expanding $1/\langle\hat{l}_1 i\rangle$ in $1/z$ to obtain the $\mathcal{O}(z^0)$ piece at $z \to \infty$.

We can remove the poles of type (1) by choosing $|\alpha\rangle = |a\rangle$, since the factor of $\langle l_2, a\rangle$ in the numerator of Eq. (B1) will cancel this pole. Thus the only contributions remaining are of types (2) and (3). We rewrite Eq. (B1) such that each type of pole is separated:

$$\begin{aligned}S_{a,b}^{(i,j)} = A_n^{\text{tree}}&\frac{\langle b, \hat{l}_1\rangle^3}{\langle l_1, l_2\rangle^2}\left\{\frac{\langle i, b\rangle}{\langle\hat{l}_1, i\rangle} - \frac{\langle i+1, b\rangle}{\langle\hat{l}_1, i+1\rangle}\right\}\\ &\times\left\{\frac{\langle j, a\rangle}{\langle l_2, j\rangle} - \frac{\langle j+1, a\rangle}{\langle l_2, j+1\rangle}\right\}\left(\frac{-\langle a, l_2\rangle^3}{\langle a, b\rangle^4}\right).\end{aligned}$$

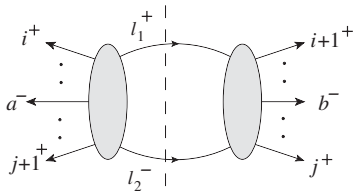

FIG. 18. The (l_1^+, l_2^-) helicity configuration for the two-particle cut $(j+1, \ldots, a, \ldots, i|i+1, \ldots, b, \ldots, j)$ of $A_n^{\text{MHV}}(a^-, b^-)$.

Next, we expand around $z \to \infty$ obtaining

$$\begin{aligned}\mathcal{S}^{(i,j)}_{a,b}(\lambda) &\equiv S^{(i,j)}_{a,b}|_{\mathcal{O}(z^0)} \\ &= A^{\text{tree}}_n\{\mathcal{G}^{(i,j)}_{a,b,i}(\lambda) - \mathcal{G}^{(i,j)}_{a,b,i+1}(\lambda)\}\left\{\frac{\langle j,a\rangle}{\langle\lambda,j\rangle} - \frac{\langle j+1,a\rangle}{\langle\lambda,j+1\rangle}\right\}\left(\frac{-\langle a,\lambda\rangle^3}{\langle a,b\rangle^4}\right), \\ &= A^{\text{tree}}_n\{I\}\{J\}\left(\frac{-\langle a,\lambda\rangle^3}{\langle a,b\rangle^4}\right),\end{aligned} \tag{B2}$$

where we have used $\{I\}$ and $\{J\}$ as a shorthand notation for the terms in the curly brackets. Later we will see manifest cancellation of CCP for the terms in $\{I\}$ under the summation over the i indices, and similarly for $\{J\}$ under the summation over the j indices. The new functional $\mathcal{G}^{(i,j)}_{a,b,i}$ is defined as

$$\begin{aligned}\mathcal{G}^{(i,j)}_{a,b,i} &\equiv \frac{\langle i,b\rangle}{\langle l_1,l_2\rangle^2}\frac{\langle b,\hat{l}_1\rangle^3}{\langle\hat{l}_1,i\rangle}\Big|_{\mathcal{O}(1)} = \frac{\langle i,b\rangle}{\langle l_1,l_2\rangle^2}\left(3\frac{\langle b,l_1\rangle^2\langle b,l_2\rangle}{\langle l_2,i\rangle} - 3\frac{\langle b,l_1\rangle\langle b,l_2\rangle^2\langle l_1,i\rangle}{\langle l_2,i\rangle^2} + \frac{\langle b,l_2\rangle^3\langle l_1,i\rangle^2}{\langle l_2,i\rangle^3}\right) \\ &= \frac{\langle i,b\rangle}{\langle\lambda|P_{i,j}|\lambda]^2}\left(3\frac{\langle b|P_{i,j}|\lambda]^2\langle b,\lambda\rangle}{\langle\lambda,i\rangle} + 3\frac{\langle b|P_{i,j}|\lambda]\langle b,\lambda\rangle^2\langle i|P_{i,j}|\lambda]}{\langle\lambda,i\rangle^2} + \frac{\langle b,\lambda\rangle^3\langle i|P_{i,j}|\lambda]^2}{\langle\lambda,i\rangle^3}\right),\end{aligned} \tag{B3}$$

and similarly,

$$\mathcal{G}^{(i,j)}_{a,b,i+1} \equiv \frac{\langle i+1,b\rangle}{\langle\lambda|P_{i,j}|\lambda]^2}\left(3\frac{\langle b|P_{i,j}|\lambda]^2\langle b,\lambda\rangle}{\langle\lambda,i+1\rangle} + 3\frac{\langle b|P_{i,j}|\lambda]\langle b,\lambda\rangle^2\langle i+1|P_{i,j}|\lambda]}{\langle\lambda,i+1\rangle^2} + \frac{\langle b,\lambda\rangle^3\langle i+!|P_{i,j}|\lambda]^2}{\langle\lambda,i+1\rangle^3}\right). \tag{B4}$$

Note the function $\mathcal{G}^{i,j}_{a,b,i}(\lambda)$ has higher-order (aka not simple) collinear poles in $\langle\lambda,i\rangle$, which will require extra care in using the holomorphic anomaly as we later discuss.

The dLIPS integral of (B2) is localized by the four poles appearing in the curly brackets, and it will be convenient to separate the contributions from the first and second curly brackets. Writing

$$\sum_{i,j}\frac{-1}{2\pi i}\int d\text{LIPS}\mathcal{S}^{(i,j)}_{a,b}(\lambda) = \sum_{i,j}\frac{-1}{2\pi i}\int d\text{LIPS}[\mathcal{S}^{(i,j)}_{a,b}(\lambda)|_{\{J\}} + \mathcal{S}^{(i,j)}_{a,b}(\lambda)|_{\{I\}}], \tag{B5}$$

where $|_{\{I\}}$ indicates the contributions that arise from the presence of poles in $\{I\}$. We first consider the sum of residues of the simple poles $1/\langle\lambda,j\rangle$ and $1/\langle\lambda,j+1\rangle$ in the second curly brackets:

$$\begin{aligned}\sum_{i,j}\mathcal{S}^{(i,j)}_{a,b}(\lambda)|_{\{J\}} &= \sum_{i,j}A^{\text{tree}}_n\{\mathcal{G}^{(i,j)}_{a,b,i}(\lambda) - \mathcal{G}^{(i,j)}_{a,b,i+1}(\lambda)\}\left\{\frac{\langle j,a\rangle}{\langle\lambda,j\rangle}\right\}\left(\frac{-\langle a,\lambda\rangle^3}{\langle a,b\rangle^4}\right)\Big|_{\langle l,j\rangle} \\ &\quad - \sum_{i,j}A^{\text{tree}}_n\{\mathcal{G}^{(i,j)}_{a,b,i}(\lambda) - \mathcal{G}^{(i,j)}_{a,b,i+1}(\lambda)\}\left\{\frac{\langle j+1,a\rangle}{\langle\lambda,j+1\rangle}\right\}\left(\frac{-\langle a,\lambda\rangle^3}{\langle a,b\rangle^4}\right)\Big|_{\langle\lambda,j+1\rangle} \\ &= \sum_{i,j}A^{\text{tree}}_n\{\mathcal{G}^{(i,j)}_{a,b,i}(\lambda) - \mathcal{G}^{(i,j)}_{a,b,i+1}(\lambda)\}\left\{\frac{\langle j,a\rangle}{\langle\lambda,j\rangle}\right\}\left(\frac{-\langle a,\lambda\rangle^3}{\langle a,b\rangle^4}\right)\Big|_{\langle\lambda,j\rangle} \\ &\quad - \sum_{i,j'}A^{\text{tree}}_n\{\mathcal{G}^{(i,j'-1)}_{a,b,i}(\lambda) - \mathcal{G}^{(i,j'-1)}_{a,b,i+1}(\lambda)\}\left\{\frac{\langle j',a\rangle}{\langle\lambda,j'\rangle}\right\}\left(\frac{-\langle a,\lambda\rangle^3}{\langle a,b\rangle^4}\right)\Big|_{\langle\lambda,j'\rangle},\end{aligned} \tag{B6}$$

where we have used $|_{\langle\lambda,j\rangle}$ to indicate the collinear pole on which the integrand will be localized. From (B3), we see that $\mathcal{G}^{(i,j)}_{a,b,i}(\lambda) = \mathcal{G}^{(i,j-1)}_{a,b,i}(\lambda)$ when localized at $\lambda \to j$.[12] Treating j and j' as dummy variables, the two summations simply cancel with each other and one is left with zero. Of course this is the wrong result and the subtlety lies in the summation limits. We will discuss the limits in detail in the next subsection. For now, we will show the same cancellation occurs for the higher-order poles in the first curly brackets.

The contributions from the poles in the first curly brackets in (B2) can be written as

[12]This again can be seen from the fact that on the pole, $P_{i,j}|j] = P_{i,j-1}|j]$.

$$\begin{aligned}\sum_{i,j}\mathcal{S}^{(i,j)}_{a,b}(\lambda)|_{\{I\}} &= \sum_{j,i}A_n^{\text{tree}}\{\mathcal{G}^{(i,j)}_{a,b,i}(\lambda)\}\left\{\frac{\langle j,a\rangle}{\langle\lambda,j\rangle}-\frac{\langle j+1,a\rangle}{\langle\lambda,j+1\rangle}\right\}\left(\frac{-\langle a,\lambda\rangle^3}{\langle a,b\rangle^4}\right)\Big|_{\langle\lambda,i\rangle}\\ &\quad-\sum_{j,i}A_n^{\text{tree}}\{\mathcal{G}^{(i,j)}_{a,b,i+1}(\lambda)\}\left\{\frac{\langle j,a\rangle}{\langle\lambda,j\rangle}-\frac{\langle j+1,a\rangle}{\langle\lambda,j+1\rangle}\right\}\left(\frac{-\langle a,\lambda\rangle^3}{\langle a,b\rangle^4}\right)\Big|_{\langle\lambda,i+1\rangle}\\ &= \sum_{j,i}A_n^{\text{tree}}\{\mathcal{G}^{(i,j)}_{a,b,i}(\lambda)\}\left\{\frac{\langle j,a\rangle}{\langle\lambda,j\rangle}-\frac{\langle j+1,a\rangle}{\langle\lambda,j+1\rangle}\right\}\left(\frac{-\langle a,\lambda\rangle^3}{\langle a,b\rangle^4}\right)\Big|_{\langle\lambda,i\rangle}\\ &\quad-\sum_{j,i'}A_n^{\text{tree}}\{\mathcal{G}^{(i'-1,j)}_{a,b,i'}(\lambda)\}\left\{\frac{\langle j,a\rangle}{\langle\lambda,j\rangle}-\frac{\langle j+1,a\rangle}{\langle\lambda,j+1\rangle}\right\}\left(\frac{-\langle a,\lambda\rangle^3}{\langle a,b\rangle^4}\right)\Big|_{\langle\lambda,i'\rangle}.\end{aligned} \tag{B7}$$

Here, the integral will be localized by the poles that are present in $\mathcal{G}^{(i,j)}_{a,b,i}(\lambda)$, which besides simple poles, has higher-order poles at the same kinematic point. Repeated use of the Schouten identity allows one to extra the contribution of the higher-order poles to the simple pole [27], which we review in Appendix A. Denoting the resulting expression as $\mathcal{H}^{(i,j)}_{a,b,i}(\lambda)$, we have

$$\sum_{i,j}\mathcal{S}^{(i,j)}_{a,b}(\lambda)|_{\{I\}} = \sum_{j,i}\frac{A_n^{\text{tree}}}{\langle a,b\rangle^4}\{\mathcal{H}^{(i,j)}_{a,b,i}(\lambda)-\mathcal{H}^{(i,j+1)}_{a,b,i}(\lambda)-\mathcal{H}^{(i-1,j)}_{a,b,i}(\lambda)+\mathcal{H}^{(i-1,j+1)}_{a,b,i}(\lambda)\}|_{\langle\lambda,i\rangle}. \tag{B8}$$

The explicit form of $\mathcal{H}^{(i,j)}_{a,b,i}(\lambda)$ is given in Eq. (B14). The key fact of $\mathcal{H}^{(i,j)}_{a,b,i}(\lambda)$ and $\mathcal{H}^{(i-1,j)}_{a,b,i}(\lambda)$ is that they become identical when the integrand is evaluated on the pole $1/\langle\lambda,i\rangle$ and integrated on the real contour $\tilde{\lambda}=\bar{\lambda}$. Therefore Eq. (B8) again gives zero.

While the limits of the summation require careful treatment, our analysis shows that indeed for nonadjacent MHV, the cancellation of CCP again reduces the sum of bubble coefficients to a few terminal terms which we will now identify.

1. *d*LIPS integrals of higher-order poles

As we have seen, generic pole terms in nonadjacent MHV bubble coefficients' $g(\lambda)$'s generically have higher-order poles. We evaluate the integrands in a manner following that in Sec. 2.3 of Ref. [27]. Specifically, the *d*LIPS integrands are rational functions of λ of degree -2. We can recursively reduce the degree of λ in the numerator and denominator by one unit each, through repeated application of the following Schouten identity [27]:

$$\frac{\langle a,\lambda\rangle}{\langle\beta,\lambda\rangle\langle\gamma,\lambda\rangle}=\frac{\langle a,\beta\rangle}{\langle\gamma,\beta\rangle}\frac{1}{\langle\beta,\lambda\rangle}+\frac{\langle a,\gamma\rangle}{\langle\beta,\gamma\rangle}\frac{1}{\langle\gamma,\lambda\rangle}. \tag{B9}$$

Repeated application reduces integrands with higher-order poles to sums of integrands with either simple poles, or to multiple poles, such as $1/\langle a,\lambda\rangle^2$, $\langle x,\lambda\rangle/\langle a,\lambda\rangle^3$, etc., with trivial residues as $|\lambda\rangle\to|a\rangle$. The generic forms for the residues at second- and third-order poles are

$$\frac{1}{\langle\beta,\lambda\rangle^2}\prod_{i=1}^n\frac{\langle a_i,\lambda\rangle}{\langle b_i,\lambda\rangle}\Big|_{\langle\lambda,\beta\rangle}=\prod_{i=1}^n\frac{\langle a_i,\beta\rangle}{\langle b_i,\beta\rangle}\sum_{1\le i\le n}\frac{\langle a_i,b_i\rangle}{\langle a_i,\beta\rangle\langle b_i,\beta\rangle}, \tag{B10}$$

$$\frac{\langle\xi,\lambda\rangle}{\langle\beta,\lambda\rangle^3}\prod_{i=1}^n\frac{\langle a_i,\lambda\rangle}{\langle b_i,\lambda\rangle}\Big|_{\langle\lambda,\beta\rangle}=\langle\xi,\beta\rangle\prod_{i=1}^n\frac{\langle a_i,\beta\rangle}{\langle b_i,\beta\rangle}\left\{\sum_{1\le i\le j\le n}\frac{\langle a_i,b_i\rangle}{\langle a_i,\beta\rangle\langle b_i,\beta\rangle}\frac{\langle a_j,b_j\rangle}{\langle a_j,\beta\rangle\langle b_j,\beta\rangle}+\sum_{1\le k\le n}\frac{\langle a_k,b_k\rangle}{\langle a_k,\beta\rangle\langle b_k,\beta\rangle}\frac{\langle a_k,\xi\rangle}{\langle\xi,\beta\rangle\langle a_k,\beta\rangle}\right\}. \tag{B11}$$

With this, we can factor out the irrelevant multiple poles in any expression, for example we have the following rewriting:

$$\frac{\langle b,\lambda\rangle^2\langle\lambda,a\rangle^3}{\langle\lambda,i\rangle^2\langle\lambda,j\rangle\langle\lambda|P_{i,j}|\lambda]^4}\Big|_{\langle\lambda,i\rangle}=-\frac{\langle i,a\rangle^3\langle i,b\rangle^2\left(\frac{2\langle a|P_{i,j}|i]}{\langle i|P_{i,j}|i]\langle i,a\rangle}+\frac{2\langle b|P_{i,j}|i]}{\langle i|P_{i,j}|i]\langle i,b\rangle}+\frac{\langle a,j\rangle}{\langle i,a\rangle\langle i,j\rangle}\right)}{\langle i|P_{i,j}|i]^4\langle i,j\rangle}, \tag{B12}$$

$$\frac{\langle\lambda,a\rangle^3\langle b,\lambda\rangle^3}{\langle\lambda,j\rangle\langle\lambda,i\rangle^3\langle\lambda|P_{i,j}|\lambda]^4}\Big|_{\langle\lambda,i\rangle}=\frac{\langle a,i\rangle^3\langle b,i\rangle^3}{\langle i|P_{i,j}|i]^4\langle i,j\rangle}\Big(\frac{3\langle a|P_{i,j}|i]^2}{\langle i|P_{i,j}|i]^2\langle a,i\rangle^2}+\frac{3\langle b|P_{i,j}|i]^2}{\langle i|P_{i,j}|i]^2\langle b,i\rangle^2}+\frac{2\langle a|P_{i,j}|i]\langle a,b\rangle}{\langle i|P_{i,j}|i]\langle a,i\rangle^2\langle b,i\rangle}$$
$$+\frac{4\langle a|P_{i,j}|i\rangle\langle b|P_{i,j}|i]}{\langle i|P_{i,j}|i]^2\langle a,i\rangle\langle b,i\rangle}+\frac{\langle a,j\rangle^2}{\langle a,i\rangle^2\langle i,j\rangle^2}+\frac{2\langle a|P_{i,j}|i]\langle a,j\rangle}{\langle i|P_{i,j}|i]\langle a,i\rangle^2\langle i,j\rangle}+\frac{\langle a,b\rangle\langle a,j\rangle}{\langle a,i\rangle^2\langle b,i\rangle\langle i,j\rangle}$$
$$+\frac{2\langle b|P_{i,j}|i]\langle a,j\rangle}{\langle i|P_{i,j}|i]\langle a,i\rangle\langle b,i\rangle\langle i,j\rangle}\Big). \tag{B13}$$

Combining these results, we can rewrite $\mathcal{G}^{(i,j)}_{a,b,i}(\lambda)\frac{\langle\lambda,a\rangle^3\langle j,a\rangle}{\langle\lambda|P_{i,j}|\lambda]^2\langle\lambda,j\rangle}$ to $\mathcal{H}^{(i,j)}_{a,b,i}$ as in (B8):

$$\mathcal{G}^{(i,j)}_{a,b,i}(\lambda)\frac{\langle\lambda,a\rangle^3\langle j,a\rangle}{\langle\lambda|P_{i,j}|\lambda]^2\langle\lambda,j\rangle}\Big|_{\langle\lambda,i\rangle}=\frac{\langle i,a\rangle^3\langle j,a\rangle}{\langle i,j\rangle}\langle i,b\rangle\Big(3\frac{\langle b|P_{i,j}|i]^2\langle b,i\rangle}{\langle\lambda|P_{i,j}|\lambda]^2}+3\langle j,a\rangle\langle b|P_{i,j}|i]\langle i|P_{i,j}|i]\times\text{(B.12)}$$
$$+\langle j,a\rangle\langle i|P_{i,j}|i]^2\times\text{(B.13)}\Big). \tag{B14}$$

The upshot is that (B14) has vanishing residue at the poles $\lambda=a$ and $\lambda=b$. Note that if one considers $\mathcal{H}^{(i-1,j)}_{a,b,i}$, the only difference is substituting $P_{i,j}$ in $\mathcal{H}^{(i,j)}_{a,b,i}$ with $P_{i-1,j}$. It can be easily seen that on the pole $1/\langle\lambda,i\rangle$, the two are equivalent.

2. Terminal poles, terminal cuts, and their evaluation

In determining the limits of the summation, one has to avoid configurations where there is a 3-point amplitude one side of the cut, as these produce massless bubbles that are set to zero in dimensional regularization. This implies that in the summation of i, j in Eqs. (B6) and (B8), the summation limit of one index will depend on the value of the other.

For Eq. (B6) one sums over the index j first, and the limit is given as

$$\sum_{i,j}=\sum_{i=a+1}^{b-2}\sum_{j=b}^{a-1}+\sum_{j=b+1}^{a-1}\Big|_{i=b-1}+\sum_{j=b}^{a-2}\Big|_{i=a}, \tag{B15}$$

where $|_{i=b-1}$ indicates the index i is held fixed to be $b-1$. Using $j'=j+1$, the summation limit for j' is given as

$$\sum_{i,j'=j+1}=\sum_{i=a+1}^{b-2}\sum_{j'=b+1}^{a}+\sum_{j'=b+2}^{a}\Big|_{i=b-1}+\sum_{j'=b+1}^{a-1}\Big|_{i=a}. \tag{B16}$$

Looking back at Eq. (B6) we see that there are mismatches in the limits between two sums, and hence the cancellation is not complete, leaving behind

$$\sum_{i=a+1}^{b-2}X^{(i,j)}_{a,b}|_{j=b}-\sum_{i=a+1}^{b-2}X^{(i,j')}_{a,b}|_{j'=a}+X^{(i,j)}_{a,b}|^{i=b-1}_{j=b+1}$$
$$-X^{(i,j')}_{a,b}|^{i=b-1}_{j'=a}+X^{(i,j)}_{a,b}|^{i=a}_{j=b}-X^{(i,j')}_{a,b}|^{i=a}_{j'=a-1}, \tag{B17}$$

where $X^{(i,j)}_{a,b}=-A^{\text{tree}}_n\{\mathcal{G}^{(i,j)}_{a,b,i}(\lambda)-\mathcal{G}^{(i,j)}_{a,b,i+1}(\lambda)\}\frac{\langle j,a\rangle}{\langle\lambda,j\rangle}\frac{\langle a,\lambda\rangle^3}{\langle a,b\rangle^4}|_{\langle\lambda,j\rangle}$. The first two terms in Eq. (B17) evaluate to zero. To see this note that these two sums are evaluated on the pole $1/\langle\lambda,b\rangle$ and $1/\langle\lambda,a\rangle$ respectively. Looking at the summand in Eq. (B6) there is a factor $\langle\lambda,a\rangle$ in the numerator while $\mathcal{G}^{(i,j)}_{a,b,i}$ has at least one $\langle\lambda,b\rangle$ in the numerator, as can be seen from Eq. (B3). For the same reason, the fourth and fifth terms vanish as well. The remaining terms are given by

$$\sum_{i,j}\mathcal{S}^{(i,j)}_{a,b}(\lambda)|_{\{J\}}$$
$$=A^{\text{tree}}_n\{\mathcal{G}^{(b-1,b+1)}_{a,b,b-1}(\lambda)-\mathcal{G}^{(b-1,b+1)}_{a,b,b}(\lambda)\}$$
$$\times\Big\{\frac{\langle b+1,a\rangle}{\langle\lambda,b+1\rangle}\Big\}\Big(\frac{-\langle a,\lambda\rangle^3}{\langle a,b\rangle^4}\Big)\Big|_{\langle\lambda,b+1\rangle}-A^{\text{tree}}_n\{\mathcal{G}^{(a,a-2)}_{a,b,a}(\lambda)$$
$$-\mathcal{G}^{(a,a-2)}_{a,b,a+1}(\lambda)\}\Big\{\frac{\langle a-1,a\rangle}{\langle\lambda,a-1\rangle}\Big\}\Big(\frac{-\langle a,\lambda\rangle^3}{\langle a,b\rangle^4}\Big)\Big|_{\langle\lambda,a-1\rangle}. \tag{B18}$$

Therefore, we see the complicated summation (B6) reduces to only two terms: the residue at the pole $\langle\lambda,a-1\rangle=0$ in channel $(i=a,\ j=a-2)$, and the residue of the pole $\langle\lambda,b+1\rangle=0$ in channel $(i=b-1,\ j=b+1)$.

We now look at Eq. (B8), where the index i was summed first. The summation limit is given by

$$\sum_{j,i}=\sum_{j=b+1}^{a-2}\sum_{i=a}^{b-1}+\sum_{i=a+1}^{b-1}\Big|_{j=a-1}+\sum_{i=a}^{b-2}\Big|_{j=b}. \tag{B19}$$

Recalling that $i'=i+1$, the summation limit for i' is given by

$$\sum_{j,i'}=\sum_{j=b+1}^{a-2}\sum_{i'=a+1}^{b}+\sum_{i'=a+2}^{b}\Big|_{j=a-1}+\sum_{i'=a+1}^{b-1}\Big|_{j=b}. \tag{B20}$$

Again the mismatch of the summation limits for i and i' leads to uncanceled terms in Eq. (B8), given by

$$\sum_{j=b+1}^{a-2} Y^{(i,j)}_{a,b}|_{i=a} - \sum_{j=b+1}^{a-2} Y^{(i',j)}_{a,b}|_{i'=b} + Y^{(i,j)}_{a,b}|_{\substack{i=a+1\\ j=a-1}} - Y^{(i',j)}_{a,b}|_{\substack{i'=b\\ j=a-1}} + Y^{(i,j)}_{a,b}|_{\substack{i=a\\ j=b}} - Y^{(i',j)}_{a,b}|_{\substack{i'=b-1\\ j=b}}, \tag{B21}$$

where $Y^{(i,j)}_{a,b} = A^{\text{tree}}_n\{\mathcal{H}^{(i,j)}_{a,b,i}(\lambda) - \mathcal{H}^{(i,j+1)}_{a,b,i}(\lambda) - \mathcal{H}^{(i-1,j)}_{a,b,i}(\lambda) + \mathcal{H}^{(i-1,j+1)}_{a,b,i}(\lambda)\}/\langle a,b\rangle^4|_{\langle\lambda,i\rangle}$. The second and fourth terms in Eq. (B21) evaluate to zero since they have vanishing residue on the pole $1/\langle\lambda, b\rangle$, as can be seen from the presence of $\langle\lambda, b\rangle$ in the numerator of Eqs. (B3) and (B4). The first and fifth terms also vanish due to the $\langle\lambda, a\rangle^3$ in the numerator of Eq. (B7). As a result, the sum in Eq. (B8) reduces to

$$\sum_{i,j} \mathcal{S}^{(i,j)}_{a,b}(\lambda)|_{\{I\}} = \frac{A^{\text{tree}}_n}{\langle a,b\rangle^4}\{(\mathcal{H}^{(a+1,a-1)}_{a,b,a+1}(\lambda) - \mathcal{H}^{(a+1,a)}_{a,b,a+1}(\lambda))|_{\langle\lambda,a+1\rangle} - (\mathcal{H}^{(b-2,b)}_{a,b,b-1}(\lambda) - \mathcal{H}^{(b-2,b+1)}_{a,b,b-1}(\lambda))|_{\langle\lambda,b-1\rangle}\}. \tag{B22}$$

Thus the sum localizes to the pole $\langle\lambda, a+1\rangle = 0$ in channel $(i = a+1,\ j = a-1)$ and $\langle\lambda, b-1\rangle = 0$ in channel $(i = i'-1 = b-2,\ j = b)$.

Collecting all the pieces we now have

$$\begin{aligned}\mathcal{C}_2(l_1^+, l_2^-) = \frac{-1}{2\pi i}\int_{\tilde{\lambda}=\tilde{\lambda}} d\text{LIPS}\,\frac{A^{\text{tree}}_n}{\langle a,b\rangle^4}\Big\{&-(\mathcal{G}^{(b-1,b+1)}_{a,b,b-1}(\lambda) - \mathcal{G}^{(b-1,b+1)}_{a,b,b}(\lambda))\frac{\langle b+1,a\rangle}{\langle\lambda,b+1\rangle}\langle a,\lambda\rangle^3|_{\langle\lambda,b+1\rangle}\\ &+(\mathcal{G}^{(a,a-1)}_{a,b,a}(\lambda) - \mathcal{G}^{(a,a-1)}_{a,b,a+1}(\lambda))\frac{\langle a-1,a\rangle}{\langle\lambda,a-1\rangle}\langle a,\lambda\rangle^3|_{\langle\lambda,a-1\rangle}(\mathcal{H}^{(a+1,a-1)}_{a,b,a+1}(\lambda) - \mathcal{H}^{(a+1,a)}_{a,b,a+1}(\lambda))|_{\langle\lambda,a+1\rangle}\\ &-(\mathcal{H}^{(b-2,b)}_{a,b,b-1}(\lambda) - \mathcal{H}^{(b-2,b+1)}_{a,b,b-1}(\lambda))|_{\langle\lambda,b-1\rangle}\Big\}.\end{aligned} \tag{B23}$$

We now evaluate the integral. As discussed in Appendix A, writing the above integrand as a total derivative will always introduce a factor of $[\lambda|P|\alpha\rangle$. With the choice of $|\alpha\rangle = |a\rangle$, terms that are evaluated on the pole $1/\langle\lambda a \pm 1\rangle$ vanish since $[a \pm 1|P_{a,a\pm1}|a\rangle = 0$. Thus the cancellation of CCP and the judicious choice or reference spinor reduce the sum of the bubble coefficient for n-point MHV amplitude to simply:

$$\begin{aligned}\mathcal{C}_2(l_1^+, l_2^-) = \frac{A^{\text{tree}}_n}{\langle a,b\rangle^4}\frac{1}{2\pi i}\int_{\tilde{\lambda}=\tilde{\lambda}} d\text{LIPS}\Big\{&(\mathcal{G}^{(b-1,b+1)}_{a,b,b-1}(\lambda) - \mathcal{G}^{(b-1,b+1)}_{a,b,b}(\lambda))\frac{\langle b+1,a\rangle}{\langle\lambda,b+1\rangle}\langle a,\lambda\rangle^3|_{\langle\lambda,b+1\rangle}\\ &+(\mathcal{H}^{(b-2,b)}_{a,b,b-1}(\lambda) - \mathcal{H}^{(b-2,b+1)}_{a,b,b-1}(\lambda))|_{\langle\lambda,b-1\rangle}\Big\}.\end{aligned} \tag{B24}$$

Expanding the parentheses, there are four different terms to be evaluated. Explicit evaluation shows the first two terms sum to cancel the last term. Thus we have

$$\mathcal{C}_2(l_1^+, l_2^-) = \frac{A^{\text{tree}}_n}{\langle a,b\rangle^4}\frac{1}{2\pi i}\int_{\tilde{\lambda}=\tilde{\lambda}} d\text{LIPS}(\mathcal{H}^{(b-2,b)}_{a,b,b-1}(\lambda))|_{\lambda\to b-1} = \frac{11}{6}A^{\text{tree}}_n. \tag{B25}$$

Adding this with the same calculation for the other helicity configuration, (l_1^-, l_2^+), one obtains the desired result, $\mathcal{C}_2 = \frac{11}{3}A^{\text{tree}} = -\beta_0 A^{\text{tree}}$.

[1] L. M. Brown and R. P. Feynman, Phys. Rev. **85**, 231 (1952); G. Passarino and M. Veltman, Nucl. Phys. **B160**, 151 (1979); G. 't Hooft and M. Veltman, Nucl. Phys. **B153**, 365 (1979); R. G. Stuart, Comput. Phys. Commun. **48**, 367 (1988); R. G. Stuart and A. Gongora, Comput. Phys. Commun. **56**, 337 (1990).

[2] D. B. Melrose, Nuovo Cimento A **40**, 181 (1965); W. van Neerven and J. A. M. Vermaseren, Phys. Lett. **137B**, 241 (1984); G. J. van Oldenborgh and J. A. M. Vermaseren, Z. Phys. C **46**, 425 (1990); G. J. van Oldenborgh, Ph.D. thesis, University of Amsterdam, 1990; A. Aeppli, Ph.D. thesis, University of Zurich, 1992.

[3] Z. Bern, L. Dixon, and D. A. Kosower, Phys. Lett. B **302**, 299 (1993); **318**, 649(E) (1993); Nucl. Phys. **B412**, 751 (1994).

[4] Z. Bern, L. J. Dixon, D. C. Dunbar, and D. A. Kosower, Nucl. Phys. **B425**, 217 (1994).

[5] Z. Bern, L. J. Dixon, D. C. Dunbar, and D. A. Kosower, Nucl. Phys. **B435**, 59 (1995).

[6] W. T. Giele and E. W. N. Glover, Phys. Rev. D **46**, 1980 (1992); W. T. Giele, E. W. N. Glover, and D. A. Kosower, Nucl. Phys. **B403**, 633 (1993); Z. Kunszt, A. Signer, and Z. Trocsanyi, Nucl. Phys. **B420**, 550 (1994).

[7] L. Dixon (private communication).

[8] N. Arkani-Hamed, F. Cachazo, and J. Kaplan, J. High Energy Phys. 09 (2010) 016.
[9] H. Elvang, Y.-t. Huang, and C. Peng, J. High Energy Phys. 09 (2011) 031.
[10] S. Lal and S. Raju, Phys. Rev. D **81**, 105002 (2010).
[11] D. Forde, Phys. Rev. D **75**, 125019 (2007).
[12] R. Britto, F. Cachazo, and B. Feng, Nucl. Phys. **B715**, 499 (2005); R. Britto, F. Cachazo, B. Feng, and E. Witten, Phys. Rev. Lett. **94**, 181602 (2005).
[13] F. Cachazo, P. Svrcek, and E. Witten, J. High Energy Phys. 09 (2004) 006.
[14] B. Feng, J. Wang, Y. Wang, and Z. Zhang, J. High Energy Phys. 01 (2010) 019.
[15] S. J. Parke and T. R. Taylor, Phys. Rev. Lett. **56**, 2459 (1986).
[16] A. Ferber, Nucl. Phys. **B132**, 55 (1978).
[17] N. Arkani-Hamed and J. Kaplan, J. High Energy Phys. 04 (2008) 076.
[18] L. J. Dixon, J. M. Henn, J. Plefka, and T. Schuster, J. High Energy Phys. 01 (2011) 035.
[19] L. J. Dixon, arXiv:hep-ph/9601359.
[20] K. Risager, J. High Energy Phys. 12 (2005) 003.
[21] H. Elvang, D. Z. Freedman, and M. Kiermaier, J. High Energy Phys. 06 (2009) 068.
[22] G. 't Hooft and M. J. G. Veltman, Ann. Poincare Phys. Theor. A **20**, 69 (1974).
[23] H. Kawai, D. C. Lewellen, and S. H. H. Tye, Nucl. Phys. **B269**, 1 (1986).
[24] Z. Bern, J. J. M. Carrasco, and H. Johansson, Phys. Rev. Lett. **105**, 061602 (2010).
[25] Z. Bern, J. J. M. Carrasco, and H. Johansson, Phys. Rev. Lett. **105**, 061602 (2010); Z. Bern, T. Dennen, Y. -t. Huang, and M. Kiermaier, Phys. Rev. D **82**, 065003 (2010).
[26] Z. Bern, J. J. Carrasco, D. Forde, H. Ita, and H. Johansson, Phys. Rev. D **77**, 025010 (2008).
[27] R. Britto, B. Feng, and P. Mastrolia, Phys. Rev. D **73**, 105004 (2006).